Application of Immunohistochemistry in Undifferentiated Neoplasms

A Practical Approach

Shivani R. Kandukuri, MD; Fan Lin, MD, PhD; Lizhen Gui, MD, PhD; Yun Gong, MD; Fang Fan, MD, PhD; Longwen Chen, MD, PhD; Guoping Cai, MD, PhD; Haiyan Liu, MD

• ***Context.***—**Advances in interventional technology have enhanced the ability to safely sample deep-seated suspicious lesions by fine-needle aspiration procedures. These procedures often yield scant amounts of diagnostic material, yet there is an increasing demand for the performance of more ancillary tests, especially immunohistochemistry and, not infrequently, molecular assays, to increase diagnostic sensitivity and specificity. A systematic approach to conserving diagnostic material is the key, and our previously proposed algorithm can be applied aptly in this context.**

Objective.—**To elaborate a simple stepwise approach to the evaluation of cytology fine-needle aspiration specimens and small biopsy tissue specimens, illustrating the algorithmic application of small panels of immunohistochemical stains in providing an accurate diagnosis with scant amounts of tissue, including the potential pitfalls that may arise while using immunohistochemical staining on small quantities of tissue.**

Data Sources.—**The sources include literature (PubMed), the first Chinese American Pathologists Association Diagnostic Pathology Course material, and the review authors' research data as well as practice experience. Seven examples selected from the CoPath database at Geisinger Medical Center (Danville, Pennsylvania) are illustrated.**

Conclusions.—**A stepwise approach to the evaluation of fine-needle aspiration and small biopsy tissue specimens in conjunction with a small panel of select immunohistochemical stains has been successful in accurately assessing the lineage/origin of the metastatic tumors of unknown primaries. The awareness of the common pitfalls of these biomarkers is essential in many instances.**

(*Arch Pathol Lab Med.* 2017;141:1014–1032; doi: 10.5858/arpa.2016-0518-RA)

Advances in interventional technology have enhanced the ability to safely sample deep-seated suspicious lesions by fine-needle aspiration (FNA) procedures as well as core needle biopsies. In addition, the discovery of specific genomic alterations in tumors has led to the development of targeted therapy, which has heightened the practice of pathology tremendously. The challenges in the practice of cytopathology and histopathology at the current time are the scant amount of diagnostic material/tissue yielded by these techniques and the demand for accurate, specific diagnosis in an era of personalized medicine. The cell block sections are potential materials for performing immunohistochemistry (IHC) and molecular tests, not only to determine the type and origin of the tumor, but also to provide genomic information to guide initial management and personalized patient care. Currently the expectations are: accurate tumor diagnosis with a site of origin, subclassification of the malignancy, and preservation of an adequate amount of tissue for possible molecular profiling. With the identification of new targets for chemotherapy that are easily assessed using fluorescence in situ hybridization testing on the cell block sections, the value of a cell block in providing personalized patient care cannot be understated.

The performance of an FNA and production of a cell block are convenient and cost-effective methods. Along with smears of aspirated cellular material are also small amounts of tumor in the form of minute "skinny" core needle biopsies in the cell blocks. A systematic approach is necessary to evaluate the limited tissue and to preserve as much tissue as possible for other downstream testing. Our previously proposed algorithm[1] can aptly be applied in this context.

Accepted for publication January 17, 2017.

From the Department of Laboratory Medicine, Geisinger Medical Center, Danville, Pennsylvania (Drs Kandukuri, Lin, and Liu); the Department of Pathology, Northwest Arkansas Pathology Group, Fayetteville (Dr Gui); the Department of Pathology, MD Anderson Cancer Center, Houston, Texas (Dr Gong); the Department of Pathology, The University of Kansas Medical Center, Kansas City (Dr Fan); the Department of Pathology, Mayo Clinic, Scottsdale, Arizona (Dr Chen); and the Department of Pathology, Yale University, New Haven, Connecticut (Dr Cai).

The authors have no relevant financial interest in the products or companies described in this article.

Presented at the First Chinese American Pathologists Association (CAPA) Diagnostic Pathology Course: Best Practices in Immunohistochemistry in Surgical Pathology and Cytopathology; August 22–24, 2015; Flushing, New York.

Reprint requests: Haiyan Liu, MD, Department of Laboratory Medicine, MC 19-20 Geisinger Medical Center, 100 N Academy Ave, Danville, PA 17822 (email: Hliu1@geisinger.edu).

The objectives of this paper are to (1) summarize the algorithms that discuss the approach and application of the most useful immunohistochemical panels in the accurate diagnoses of undifferentiated neoplasms/malignancies of unknown origin; (2) illustrate the utilities and pitfalls of frequently used and recently described diagnostic immunohistochemical markers; and (3) demonstrate the effectiveness of small IHC panels for the diagnosis of tumors of unknown origin by the presentation of 7 examples.

GENERAL APPROACH AND PROPOSED ALGORITHMS

At our institution, when adequate numbers of core biopsies are submitted, they are separated at the time of processing into at least 2 blocks to ensure that an adequate amount of tissue is available to perform IHC and molecular cytogenetic tests if indicated.

The general principles and strategies we use to work with cytologic smears and cell blocks containing cellular material or small tissue biopsies in cases with tumor of unknown primary are as follows: (1) formulate a differential diagnosis based on cytomorphology and cell block sections "blind" or "cold" without being aware of the clinical information; (2) review the patient's chart, including the history, physical examination, and lab evaluations, including imaging; (3) formulate the differential diagnosis based on cytohistomorphology and clinical information; (4) follow the algorithm[1] (see below) and perform the recommended small panel of immunohistochemical stains (a single stain is never recommended); (5) exclude certain diagnoses based on cytohistomorphology, IHC results, and clinical-radiologic findings; (6) be wary of and familiar with aberrant expression of tissue/organ-specific markers; (7) be cautious when the triple test (clinical, imaging, and cytohistomorphology) does not fit a specific entity; and (8) morphologic features and clinical findings are still fundamental.

As summarized above, the general approach begins with a morphologic evaluation of the adequately aspirated material, which usually helps to delineate the lineage of the tumor cells. The presence of cohesive, 3-dimensional clusters of cells with or without single cells in the background is suggestive of epithelial origin. Loosely cohesive clusters and numerous single cells with plasmacytoid or spindled appearance and a stippled nuclear chromatin pattern are suggestive of neuroendocrine differentiation. Spindle cells in general are suggestive of mesenchymal tumors. Small round blue cells with lymphoglandular bodies in the background are suggestive of a lymphoproliferative disorder. Individual plasmacytoid cells with prominent macronucleolus and granular cytoplasm, usually with some pigment, are suggestive of melanoma. If one is able to identify the lineage without too much difficulty, the neoplasm most likely is well to moderately differentiated. In these situations, organ-specific or tumor type–specific immunomarkers are indicated, and these are summarized in Table 1.

The poorly differentiated neoplasms are the entities that require more elaborate workup. Immunohistochemistry plays a critical role in identifying the cell lineage and probable site of origin. Given their undifferentiated nature, these tumors often lose the expression of tissue- or lineage-specific markers; therefore, a panel of immunohistochemical markers is usually recommended. By the same token, a lack of staining with 1 immunostain should not be regarded as conclusive evidence to exclude the corresponding specific tissue or lineage, because poorly differentiated/undifferentiated carcinomas frequently lose expression of site-specific antigens.

A screening panel consisting of cytokeratin (CK), S100, vimentin, and leukocyte common antigen (LCA) should be applied first as a general approach to a tumor of unknown origin, as illustrated in Figure 1.

When an epithelial origin is confirmed (CK^+, $S100^-$, $vimentin^{-/+}$, LCA^-), the basic panel of CK7 and CK20 will allow us to determine from which organ system the primary tumor could potentially be arising,[2] as summarized in Table 2.

A CK cocktail consisting of AE1/3 and CAM 5.2 is an effective marker for identification of epithelial lineage. CAM 5.2 identifies the low–molecular weight CKs, including CK7 and CK8, whereas AE1/3 is a cocktail that identifies both low–molecular weight and high–molecular weight CKs (pankeratin); however, it does not appear to react well to CK8 in practice. AE1/3 by itself is insufficient to exclude an epithelial lineage because positive immunoreactivity for AE1/3 alone was also reported in 111 cases (28%) of hepatocellular carcinoma, 150 cases (66%) of clear cell renal cell carcinoma, 23 cases (48%) of adrenal cortical carcinomas, and 98 cases (88%) of pulmonary small cell carcinomas (SMcCs).[3,4]

Other broad-spectrum CKs containing keratin 8 and keratin 18, such as the clones KL1, OSCAR, MAK6, and 5D3/LP3, are also popular choices as screening CKs. Because poorly differentiated carcinomas are known to be heterogeneous in their antigen expression, a combination of immunohistochemical stains may be essential to establish tumor lineage. A pitfall to keep in mind is that poorly fixed specimens may have an unpredictable pattern of staining for CK.[4–6]

In general, carcinomas express CK, whereas mesenchymal tumors express vimentin. However, there are exceptions to this rule. There are carcinomas that show loss of CK expression, carcinomas that frequently coexpress vimentin, and carcinomas that rarely express both CK and vimentin. These entities are summarized in Table 3. Vice versa, mesenchymal tumors and hematopoietic neoplasms may express epithelial markers, and these are summarized in Table 4.

Positive staining with LCA (CD45) and/or vimentin, but negative staining for S100 and CK, indicates lymphoid lineage, with high sensitivity and specificity for lymphoid malignancies.[7,8] However, a large percentage of lymphoblastic leukemias are frequently negative for LCA,[9,10] with unpredictable and frequently negative staining patterns in plasma cell dyscrasias and anaplastic hematopoietic lesions. Rare cases of LCA staining in metastatic undifferentiated and neuroendocrine carcinoma have also been reported.[11]

S100 is highly specific for melanocytic or neurogenic lesions, with both nuclear and cytoplasmic staining patterns. Sex-determining region Y box 10 (SOX10), melanoma-associated antigen recognized by T cells (Mart-1 [Melan-A]), and human melanoma black-45 (HMB-45) can all be performed to confirm melanocytic origin. Besides melanocytic lesions, positive staining with S100 with negative CK expression also suggests the possibilities of neurogenic tumors, chordoma, dendritic cell tumors, granular cell tumors, Langerhans cell tumors/histiocytosis, myoepithelial tumors, and some primary as well as metastatic carcinomas.[12]

Table 1. Organ-Specific or Tumor Type–Specific Immunohistochemical (IHC) Markers

Primary Site	IHC Markers
Lung adenocarcinoma	TTF-1, Napsin A
Breast carcinoma	GATA3, ER, GCDFP-15
Urothelial carcinoma	GATA3, uroplakin II, S100P, CK5/6, p63, CK20
Squamous cell carcinoma	P40, CK5/6, p63, SOX2
Renal cell carcinoma, clear cell type	PAX-8/PAX-2, RCCma, pVHL, KIM-1
Papillary renal cell carcinoma	P504S, RCCma, pVHL, PAX 8, KIM-1
Translocation renal cell carcinoma	TFE3
Hepatocellular carcinoma	Arginase-1, glypican-3
Adrenal cortical neoplasm	SF-1, Mart-1, inhibin-α, calretinin
Melanoma	S100, Mart-1, HMB-45, MiTF, SOX10, PNL2
Merkel cell carcinoma	CK20 (perinuclear dot staining), MCPyV
Mesothelial origin	Calretinin, WT1, D2-40, CK5/6, mesothelin
Neuroendocrine origin	Chromogranin, synaptophysin, CD56
Upper gastrointestinal tract	CDH17, CDX2, CK20
Lower gastrointestinal tract	SATB2, CDX2, CK20, CDH17
Intrahepatic cholangiocarcinoma	pVHL, CAIX
Pancreas, acinar cell carcinoma	Glypican-3, antitrypsin, Bcl10
Pancreas, ductal adenocarcinoma	MUC 5AC, CK17, maspin, S100P, IMP3
Pancreas, neuroendocrine tumor	PR, PAX-8, PDX1, CDH17, islet-1
Pancreas, solid pseudopapillary tumor	Nuclear β-catenin, loss of E-cadherin, PR, CD10, vimentin, loss of chromogranin
Prostate, adenocarcinoma	NKX3.1, PSA, PSAP, ERG
Ovarian serous carcinoma	PAX-8, ER, WT1
Ovarian clear cell carcinoma	pVHL, HNF-1B, KIM-1, PAX-8
Endometrial adenocarcinoma	PAX-8/PAX-2, ER, vimentin
Endocervical adenocarcinoma	PAX-8, p16, CEA, HPV in situ hybridization, loss of PAX-2
Thyroid follicular cell origin	TTF-1, PAX-8, thyroglobulin
Thyroid medullary carcinoma	Calcitonin, TTF-1, CEA, chromogranin
Salivary duct carcinoma	GATA3, AR, GCDFP-15, HER2
Thymic origin	PAX-8, p63, CD5
Seminoma	SALL4, LIN28, OCT4, CD117, D2-40
Yolk sac tumor	SALL4, LIN28, glypican-3, AFP
Embryonal carcinoma	SALL4, LIN28, OCT4, NANOG, CD30, SOX2
Choriocarcinoma	GATA3, β-HCG, CD10
Sex cord stromal tumor	SF-1, inhibin-α, calretinin, FOXL2
Vascular tumor	ERG, CD31, CD34, Fli-1
Synovial sarcoma	TLE1, CK
Chordoma	CK, S100, brachyury
Desmoplastic small round cell tumor	CK, CD99, desmin, WT1 (N-terminus)
Alveolar soft-part sarcoma	TFE3
Rhabdomyosarcoma	Myogenin, desmin, MyoD1
Smooth muscle tumor	SMA, MSA, desmin, calponin
Ewing sarcoma/PNET	NKX2.2, CD99, Fli-1
Myxoid and round cell liposarcoma	NY-ESO-1
Low-grade fibromyxoid sarcoma	MUC4
Epithelioid sarcoma	CD34, loss of INI1
Atypical lipomatous tumor	MDM2 (MDM2 by FISH is a more sensitive and specific test), CDK4
Histiocytosis X	CD1a, S100, langerin (CD207)
Angiomyolipoma	HMB-45, SMA, Mart-1
Gastrointestinal stromal tumor	CD117, DOG1
Solitary fibrous tumor	STAT6, CD34, Bcl2, CD99
Myoepithelial carcinoma	Cytokeratin and myoepithelial markers (may lose INI1)
Myeloid sarcoma	CD43, CD34, MPO
Follicular dendritic cell tumor	CD21, CD35
Mast cell tumor	CD117, tryptase

Abbreviations: AFP, α-fetoprotein; AR, androgen receptor; Bcl, B-cell lymphoma; β-HCG, β-human chorionic gonadotropin; CAIX, carbonic anhydrase IX; CDH17, cadherin 17; CDK4, cyclin-dependent kinase 4; CDX2, caudal type homeobox 2; CEA, carcinoembryonic antigen; CK, cytokeratin; D2-40, podoplanin; DOG1, discovered on GIST1; ER, estrogen receptor; ERG, ETS-related gene; FISH, fluorescence in situ hybridization; Fli-1, friend leukemia virus integration-1; FOXL2, forkhead box L2; GATA3, GATA-binding protein 3; GCDFP-15, gross cystic disease fluid protein 15; HER2, human epidermal receptor 2; HMB-45, human melanoma black 45; HNF-1B, hepatocyte nuclear factor 1β; HPV, human papilloma virus; IMP3, insulin-like growth factor 2 mRNA-binding protein 3; INI1, integrase interactor 1; KIM-1, kidney injury molecule 1; LIN28, abnormal cell lineage protein 28; Mart-1, melanoma antigen recognized by T cells; Maspin, mammary serine protease inhibitor; MCPyV, Merkel cell polyoma virus; MiTF, microphthalmia transcription factor; MPO, myeloperoxidase; MSA, muscle-specific actin; MUC, mucin; MyoD1, myogenic differentiation 1; NKX2.2, NK2 homeobox 2; NKX3.1, NK3 homeobox 1; NY-ESO-1, New York esophageal squamous cell carcinoma-1; OCT4, octamer-binding transcription factor 4; P504S, α-methylacyl-CoA racemase; PAX, paired box gene; PDX1, pancreatic and duodenal homeobox 1; PNL2, melanoma-associated antigen; PR, progesterone receptor; PSA, prostate-specific antigen; PSAP, prostate-specific alkaline phosphatase; pVHL, von Hippel–Lindau tumor suppressor; RCCma, renal cell carcinoma marker; S100P, placental S100; SALL4, Sal-like protein 4; SATB2, special AT-rich sequence-binding protein 2; SF-1, steroidogenic factor 1; SMA, smooth muscle actin; SOX, sex-determining region Y box; STAT6, signal transducer and activator of transcription 6; TFE3, transcription factor E3; TLE1, transducin-like enhancer of split 1; TTF-1, thyroid transcription factor 1; WT1, Wilms tumor 1.

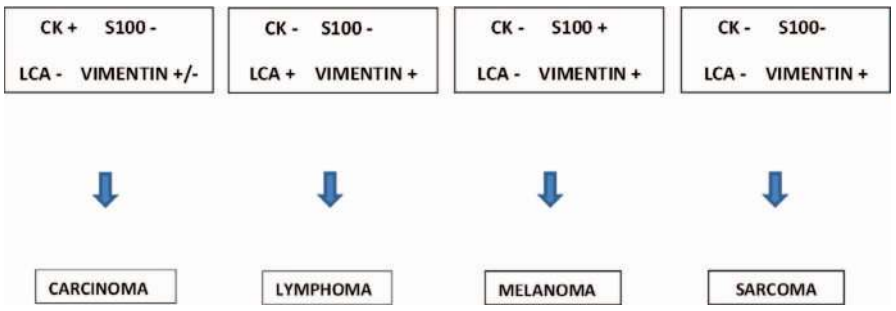

Figure 1. *The application of a suggested screening panel in tumors of unknown origin. Abbreviations: CK, cytokeratin; LCA, leukocyte common antigen.*

Vimentin is an intermediate filament characteristic of mesenchymal cells. It is found in almost all sarcomas (alveolar soft-part sarcoma tends to be negative for vimentin) and melanomas, and variably in lymphomas and even some carcinomas.[13] It is usually part of a broad panel of immunohistochemical stains and plays a supportive role in conjunction with other immunomarkers. Because the antigenicity of the tissue is preserved on optimal alcohol fixation, it also serves as an indicator of appropriate tissue fixation when positive.

THE APPLICATION OF THE ALGORITHM BY EXAMPLES

Epithelial Tumors: Metastatic Papillary Renal Cell Carcinoma, Type II

An 80-year-old man with shortness of breath was found to have mediastinal and lung masses as well as retroperitoneal lesions. Endoscopic ultrasound–guided FNA of the mediastinal mass was performed and revealed the following.

The smears revealed cohesive clusters and papillary groups of cells with enlarged round nuclei, prominent nucleoli, nuclear pleomorphism, and a moderate amount of eosinophilic, granular cytoplasm. The hematoxylin-eosin section of the cell block showed cohesive epithelial clusters of malignant cells with a moderate amount of dense eosinophilic cytoplasm on a fibrovascular core were forming papillae. Representative images are shown in Figure 2.

The assessment of cytomorphology and histomorphology suggested an epithelial neoplasm of the mediastinum that appeared to have a papillary architecture. The differential diagnosis includes primary tumors of this site, such as lung and thymic carcinomas, as well as metastases showing papillary architecture, such as thyroid, kidney, and urinary tract tumors.

The lack of nuclear grooving and pseudoinclusions of the tumor cells made thyroid papillary carcinoma less likely. The trabeculated appearance with polygonal cells and abundant cytoplasm also brought hepatocellular carcinoma and adrenal cortical carcinoma into the differential considerations. In this male patient, the presence of prominent nucleoli in the tumor cells raised the possibility of a metastatic prostate adenocarcinoma.

Immunohistochemistry studies revealed the tumor cells were positive for CK but lacked expression for CK7, CK20, and CK5/6; this CK expression phenotype made urinary and lung primaries less likely. In addition, immunostains for organ-specific immunomarkers revealed tumor cells that were positive for paired box gene 8 (PAX-8) and negative for thyroid transcription factor-1 (TTF-1) and NK3 homeobox 1 (NKX3.1). At this point, a metastatic kidney tumor was of the highest differential diagnosis consideration.

The immunostain phenotype showing negativity for CK7, CK20, CK5/6, and TTF-1 excluded lung, thyroid, and urinary tract as primary sites. Additional immunomarkers also revealed the tumor cells to be reactive to α-methylacyl-CoA racemase (P504S), patchy for von Hippel–Lindau tumor suppressor (pVHL), and focally weak for carbonic anhydrase IX (CAIX). The cytohistomorphology in conjunction with the immunostaining profile was in favor of a metastatic papillary renal cell carcinoma (PRCC). Representative images are shown in Figure 3.

The final diagnosis was consistent with metastatic PRCC, type II.

Papillary renal cell carcinoma is the second most common subtype of kidney cancer and consists of approximately 10% to 16% of cases.[14] These tumors may be bilateral or multifocal and are known to be less aggressive than RCC, clear cell type. The PRCC lesions are often red-brown and frequently have a well-demarcated pseudocapsule when small. At resection, these tumors can be either solid or have a solid and cystic appearance. They have papillary or tubulopapillary architecture and show variable proportions of papillae with frequent hemorrhage, which leads to

Table 2. Cytokeratin 7 (CK7) and CK20-Based Differential Diagnosis of Epithelial Neoplasms

	CK20$^-$	CK20$^+$
CK7$^+$	• Lung • Breast • Upper GI ADC • Pancreatic/biliary ADC • Endometrial/ endocervical ADC • Thyroid • Thymic CA • Salivary gland duct CA • Hepatocellular CA, fibrolamellar type • Ovarian serous CA • Anal duct CA • Mesothelioma	• Urothelial CA • Esophagus ADC • Gastric ADC • Small bowel ADC • Mucinous ADC of lung • Ovarian mucinous CA • Pancreaticobiliary ADC • Cholangiocarcinoma
CK7$^-$	• Hepatocellular CA • Clear cell renal cell carcinoma • Adrenal cortical CA • Prostate ADC • Small cell carcinoma • Squamous cell CA • Germ cell tumors • Neuroendocrine neoplasm • Medullary CA of the colon	• Colorectal ADC • Small bowel ADC • Bladder ADC • Merkel cell carcinoma • Appendiceal ADC • Mucinous ADC of lung • Papillary renal cell carcinoma, type II

Abbreviations: ADC, adenocarcinoma; CA, carcinoma; CK, cytokeratin; GI, gastrointestinal.

Table 3. Keratin and Vimentin Expression in Carcinomas and Mesenchymal Tumors		
Carcinomas That Frequently Express Both	**Carcinomas That Rarely Express Both**	**Mesenchymal Tumors That Frequently Express Both**
Renal cell carcinoma	Breast carcinoma	Synovial sarcoma
Anaplastic thyroid carcinoma	Ovarian carcinoma	Desmoplastic small round blue cell tumor
Endometrial carcinoma	Gastrointestinal carcinoma	Epithelioid sarcoma
Thyroid carcinoma	Lung small cell carcinoma	Epithelioid angiosarcoma
Sarcomatoid carcinoma	Lung non–small cell carcinoma	Malignant rhabdoid tumor
Mesothelioma	Prostate carcinoma	Leiomyosarcoma
Myoepithelial carcinoma		Chordoma
Metaplastic breast carcinoma		Adamantinoma

necrosis and cystic degeneration. The papillae have a central fibrovascular core with aggregates of foamy macrophages and calcifications.[15]

Papillary renal cell carcinomas have been subcategorized in to type I and type II based on morphology and immunostaining profile, as summarized in Table 5.[16–20]

For the example above, we favor a type II PRCC, based on the morphologic features of the tumor cells, such as abundant eosinophilic cytoplasm and the prominent Fuhrman grade 3 to 4 nucleoli, as well as the $CK7^{-}$ profile of this tumor.

Papillary renal cell carcinomas can be hereditary, and in these cases they are typically bilateral, multifocal, and frequently type I.[21] Cytogenetic alterations are common in PRCC. Gains of chromosomes 7, 8q, 12q, 16p, 17, and 20, and loss of 9p are often reported. The type II PRCC tumors appear to frequently gain 8q and lose 1p and 9p.[18,20]

Small Round Blue Cell Tumor–Merkel Cell Carcinoma

A 70-year-old man with a past history of colon cancer and shave biopsies for skin lesions was found to have liver masses on computed tomography scan, suspicious for metastases. An FNA of one of the liver masses was performed.

The Diff-Quik smear revealed a population of dyscohesive atypical cells with large nuclei with a fine chromatin pattern and small, inconspicuous nucleoli; a high nuclear to cytoplasmic ratio; and a very thin rim of basophilic cytoplasm in a clean background. The atypical cells were mostly single with focal nuclear molding. There were abundant mitoses and some single-cell necrosis. The Papanicolaou stain also revealed the atypical cells with a chromatin pattern suggestive of neuroendocrine differentiation. The cell block section showed clusters of small to medium-size cells with minimal cytoplasm, frequent mitoses, and apoptotic debris, similar to the findings on the smears. Representative images are shown in Figure 4.

The dyscohesive pattern of the tumor cells generated the differential considerations of a neuroendocrine neoplasm, a lymphoproliferative disorder, and melanoma. The neuroendocrine chromatin pattern and the apoptotic debris mandated the inclusion of SMcC; neuroendocrine carcinoma, large cell type; and Merkel cell carcinoma (McC) in the differential diagnosis.

Immunohistochemical stains, including CK, CK7, CK20, LCA, vimentin, S100, synaptophysin, TTF-1, and MIB-1 (Ki-67), were performed. The LCA and S100 allowed us to screen for lymphoma and melanoma. If the synaptophysin was positive, then neuroendocrine neoplasms would be considered. A mitotic index (MIB-1) in this setting would help to stratify the neuroendocrine tumors.

The tumor cells were positive for CK20 in a perinuclear dot–like pattern, CK, and synaptophysin. LCA, CK7, vimentin, S100, and TTF-1 were all negative. The MIB-1 (Ki-67) showed a proliferative index of greater than 95%. Representative images are shown in Figure 4.

The final diagnosis of this case is a metastatic McC.

Merkel cell carcinoma and SMcC share many similarities, including small blue cell morphology and neuroendocrine appearance, as well as some similarities in the staining pattern on IHC. However, there are differences between the two both morphologically and immunohistochemically. The morphologic features that may suggest McC are the slightly larger size of the cells and a less dense/more open chromatin pattern that imparts a blastlike appearance. Immunohistochemically, McC shows characteristic staining for CK20 in a perinuclear dot–like pattern secondary to the paranuclear clumping of intermediate filaments.[22]

CK20 is of critical value in the differentiation of McC from SMcC. Studies reported CK20 positivity in 97% to 100% of McCs, whereas only 1 case (8%) of SMcC was positive for CK20. TTF-1 is equally important in this differentiation. TTF-1 was reported to be positive in more than 85% of SMcCs, and no staining was seen in McCs.[22–24] Similar findings were observed in comparison of the staining pattern in McC and metastatic SMcC.[24] In addition, neurofilaments were positive in 12 McC cases (92%) and negative in all SMcCs. Other immunomarkers, such as synaptophysin, chromogranin, CD56, CK7, and neuron-specific enolase, were expressed in both with nearly the same frequency.

Table 4. Mesenchymal Tumors and Hematopoietic Neoplasms that Express Cytokeratins
Mesenchymal tumors that frequently express both
Synovial sarcoma
Desmoplastic small round blue cell tumor
Epithelioid sarcoma
Epithelioid angiosarcoma
Pleomorphic undifferentiated sarcomas
Rhabdomyosarcomas
Clear cell sarcomas
Malignant rhabdoid tumor
Leiomyosarcoma
Chordoma
Adamantinoma
Myoepithelial carcinomas
Hematopoietic tumors that express cytokeratin
Plasmacytoma
Diffuse large B-cell lymphomas
Anaplastic large cell lymphoma

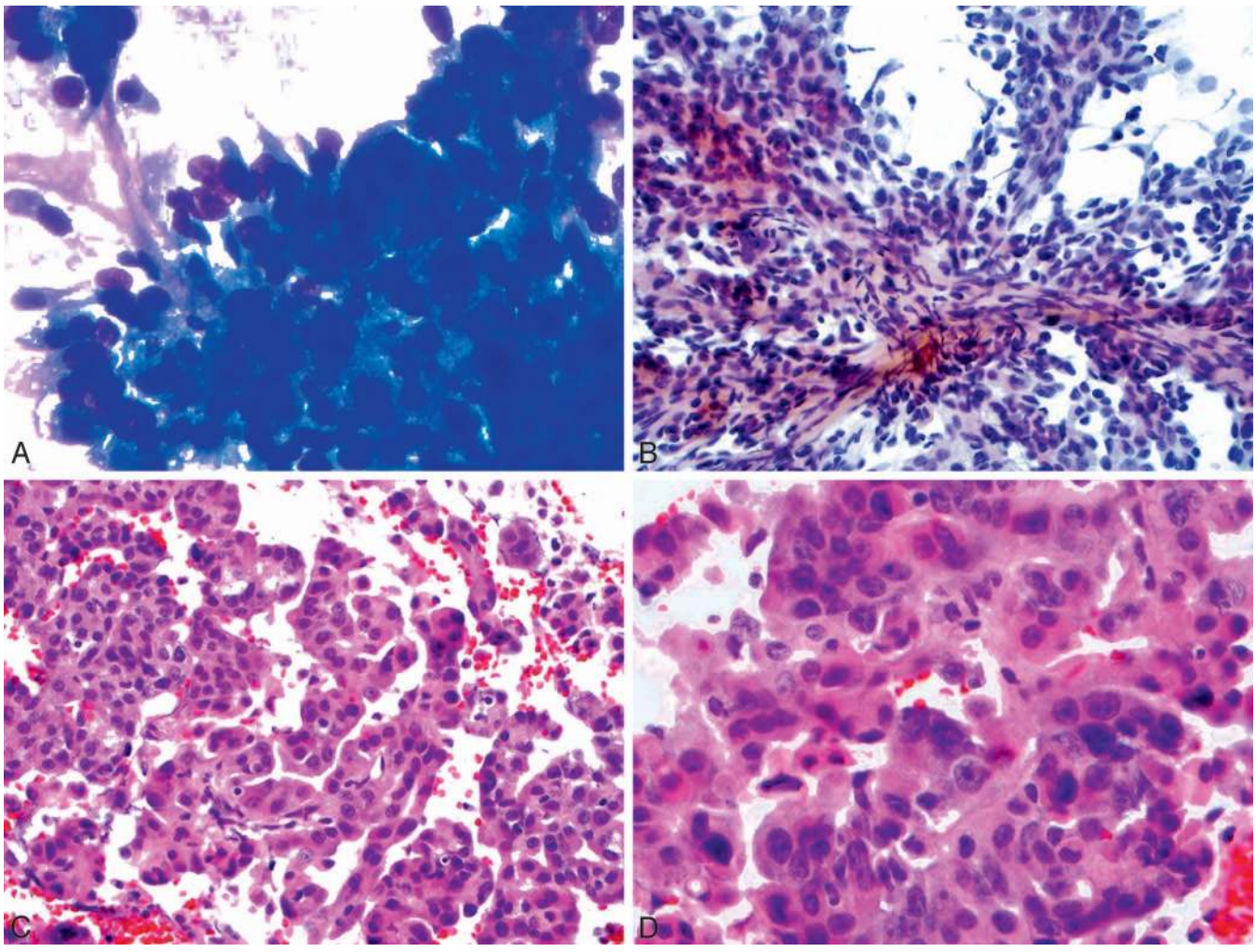

Figure 2. *Representative images of metastatic papillary renal cell carcinoma, type II. A, Cohesive clusters of tumor cells with enlarged pleomorphic nuclei, prominent nucleoli, and a moderate amount of cytoplasm. B, Papillary group of tumor cells with fibrovascular cores. C and D, Cell block sections showing cohesive groups of tumor cells with significant nuclear atypia and a moderate amount of eosinophilic and granular cytoplasm (Diff-Quik, original magnification ×400 [A]; Papanicolaou stain, original magnification ×400 [B]; hematoxylin-eosin, original magnification ×400 [C and D]).*

Mammalian or human achaete-scute complex homolog-1 (MASH1/HASH1) was reported to be a useful adjunct marker for the diagnosis of SMcC of the lung. In this study, 49 SMcC cases (83%) expressed MASH1 with a nuclear staining pattern; among those tumors, 43 cases (73%) also expressed TTF-1 along with staining of the crushed cells. It was observed that none of the 30 McCs expressed MASH1, and only 1 of the 30 McCs expressed TTF-1.[25]

Merkel cell polyomavirus (MCPyV) was identified in January 2008 by Feng et al[26] in tumor tissue from McC patients, proving clonal integration of the virus DNA into the host genome and finding prevalence of MCPyV DNA in McCs to be as high as 80% (n = 10). Since then, several studies have investigated the correlation between infection with MCPyV and clinical and prognostic factors.

Studies suggested that CK19 protein expression in tumor cells could represent functional MCPyV DNA status. Andres et al[27] found CK19 expression in 11 of 32 specimens (34%), including a $CK20^-$ McC. This expression of CK19 was seen twice as often in MCPyV DNA–negative McCs compared with MCPyV DNA–positive ones, which renders CK19 an especially useful marker in $CK20^-$ McCs.[28–31]

Unusual positivity was reported with such markers as mammary serine protease inhibitor (maspin), TTF-1, PAX-5, and terminal deoxynucleotidyl transferase (TdT).[32–34]

High-grade lymphomas, such as diffuse large B-cell lymphoma or Burkitt lymphoma, are often in the differential diagnosis because they share common cytologic or histologic features. The lymphoma cells are usually large in size, with large vesicular nuclei and prominent nucleoli that can be multiple. They usually have a moderate amount of cytoplasm that can be clear to eosinophilic to basophilic with lymphoglandular bodies in the background. A negative flow cytometry study showing a population of $CD56^+$/$CD57^-$/$CD45^-$ cells should raise concern for a malignancy of neuroendocrine origin, such as SMcC or McC.[35]

Anaplastic T-Cell Lymphoma

A 55-year-old man with a history of esophageal adenocarcinoma presented with a left axillary solid, tender

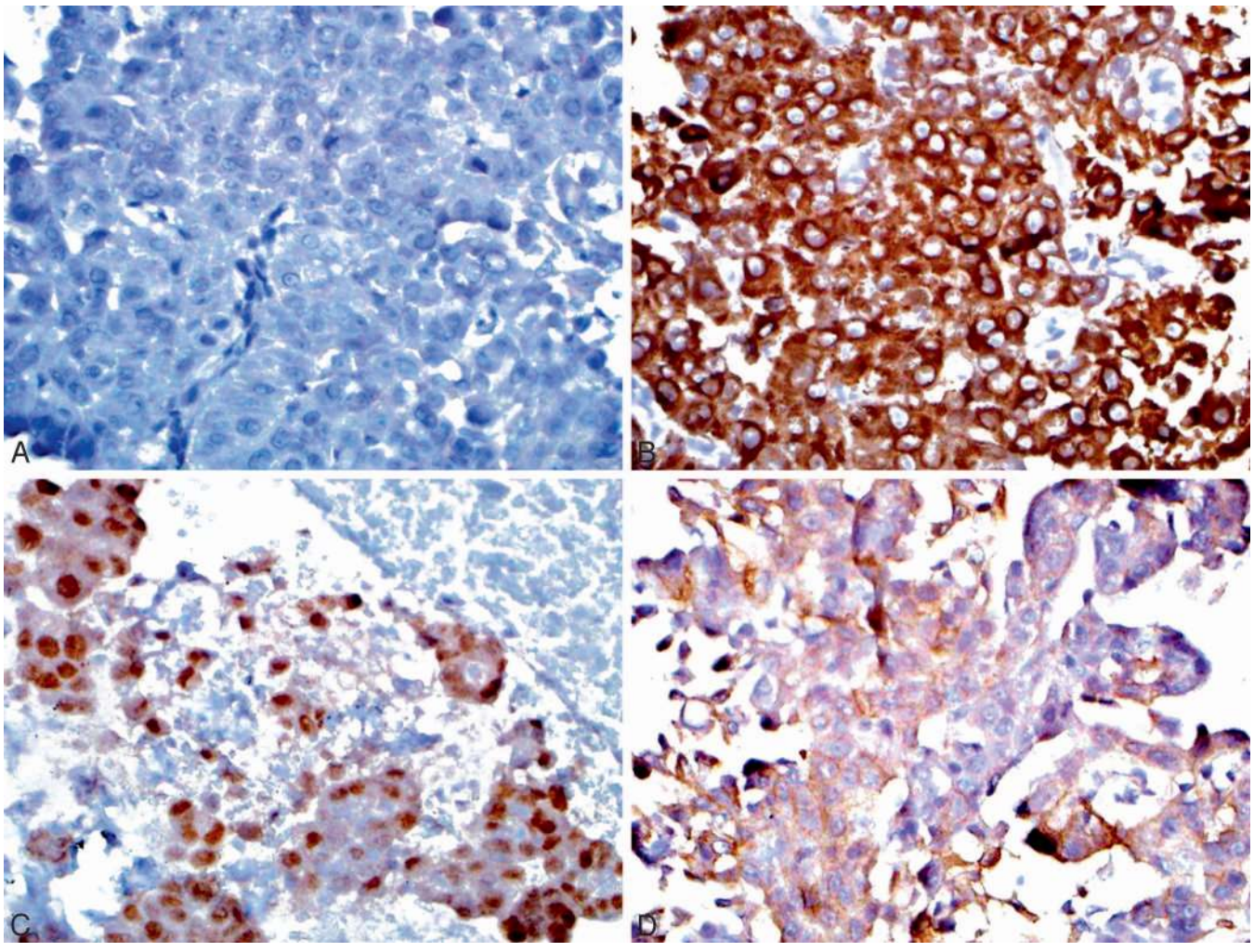

Figure 3. *Immunophenotype of metastatic papillary renal cell carcinoma, type II. A, Negative staining with cytokeratin 7 (CK7) and CK20. B, Staining with α-methylacyl-CoA racemase (P504S) was strongly positive. C, Paired box gene 8 (PAX-8) shows nuclear positivity in tumor cells. D, There is strong von Hippel–Lindau tumor suppressor (pVHL) positivity in a few tumor cells (original magnification ×400).*

mass that was greater than 5 cm in dimension. An FNA of the mass was performed.

The cellular smears were composed of a population of highly atypical cells with markedly enlarged pleomorphic nuclei and abundant eosinophilic cytoplasm. Many bizarre cells were seen showing binucleation or multinucleation, some resembling "wreath cells" or "horseshoe" or "donut-shaped" cells in the background of abundant lymphocytes, as shown in Figure 5. Frequent mitoses were also identified, whereas significant lymphoglandular bodies were not appreciated.

The presence of large, multinucleated atypical cells triggered a differential diagnosis of Hodgkin lymphoma, poorly differentiated carcinoma, anaplastic T-cell lymphoma, and pleomorphic undifferentiated sarcoma.

Immunostains with a screening panel consisting of CK, S100, vimentin, and LCA were performed and revealed the atypical cells were positive for LCA and vimentin and

Table 5. Differential Histomorphology and Immunoprofile of Papillary Renal Cell Carcinoma (PRCC)

Type I PRCC	Type II PRCC
Small basophilic cells with little cytoplasm	Large eosinophilic cells with abundant granular cytoplasm
Thin papillae lined by tumor cells in a single layer surrounding the basal membrane	Thicker papillae lined by tumor cells in pseudostratified layers
Nuclear grade usually Fuhrman grades 1–2	Nuclear grade usually Fuhrman grades 3–4
These tumors have better prognosis and longer survival	These tumors are more commonly larger, present at higher T stage and grade, and frequently have nodal or distant metastatic disease
Immunohistochemical staining is usually positive for CK7, P504S, KIM-1, and CD10	Immunohistochemical staining is frequently negative for CK7, strongly positive for P504S and CD10, and can be focally positive for CK20

Abbreviations: CK, cytokeratin; KIM-1, kidney injury molecule-1; P504S, α-methylacyl-CoA racemase.

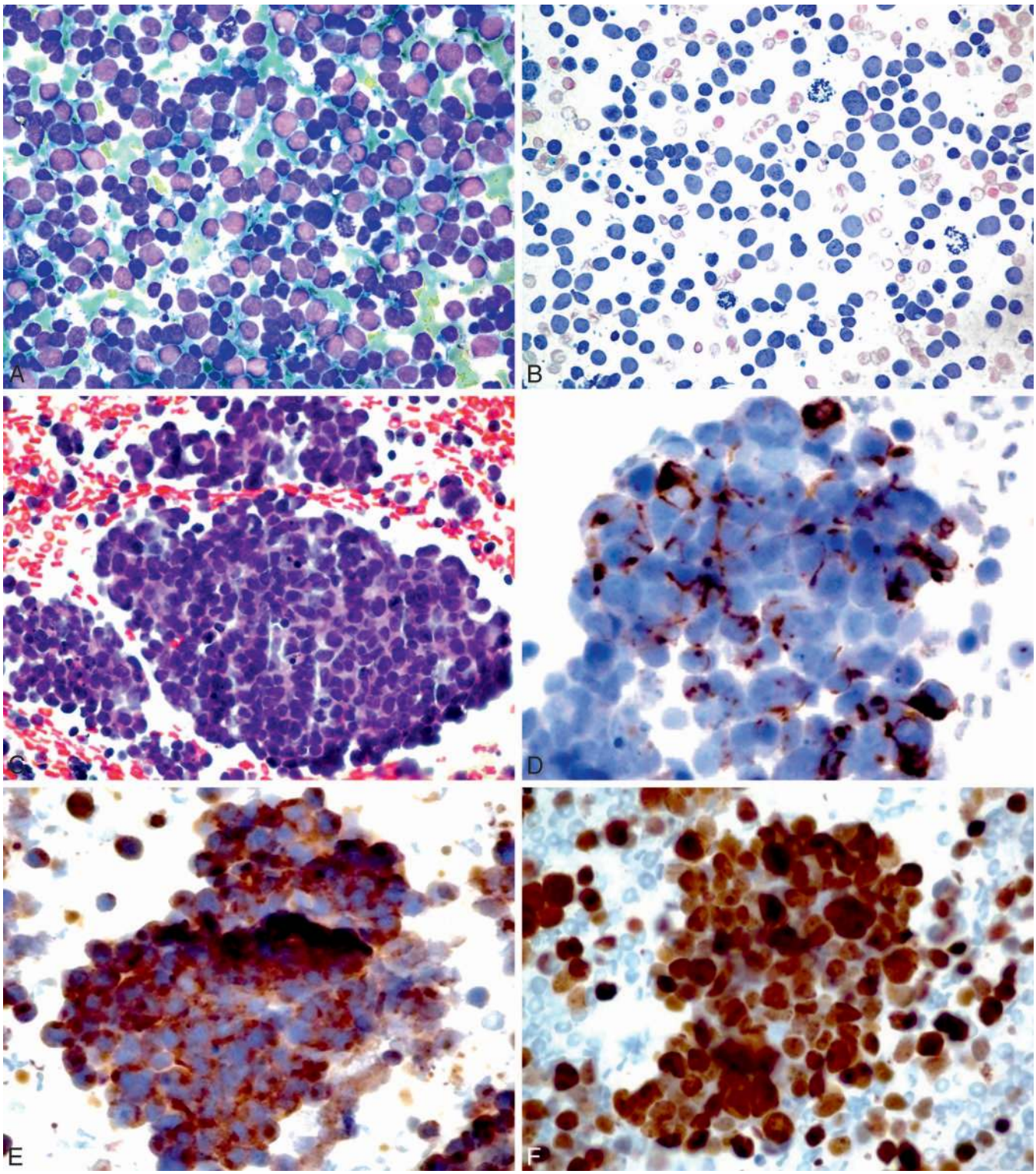

Figure 4. *Representative images of Merkel cell carcinoma. A, A population of dyscohesive atypical cells with large nuclei, high nuclear to cytoplasmic ratio, and rim of basophilic cytoplasm. B, The large nuclei with a fine chromatin pattern give an almost blastlike or neuroendocrine appearance, as well as small, inconspicuous nucleoli. C, Cell block showing clusters of medium-size cells with minimal cytoplasm, abundant nuclear apoptotic debris, and mitoses. D, Cytokeratin 20 positivity in a perinuclear dot–like pattern. E, Synaptophysin showing cytoplasmic positivity. F, MIB-1 proliferative index is higher than 95% (Diff-Quik, original magnification ×600 [A]; Papanicolaou stain, original magnification ×600 [B]; hematoxylin-eosin, original magnification ×600 [C]; immunohistochemistry, original magnifications ×400 [D and E] and ×600 [F]).*

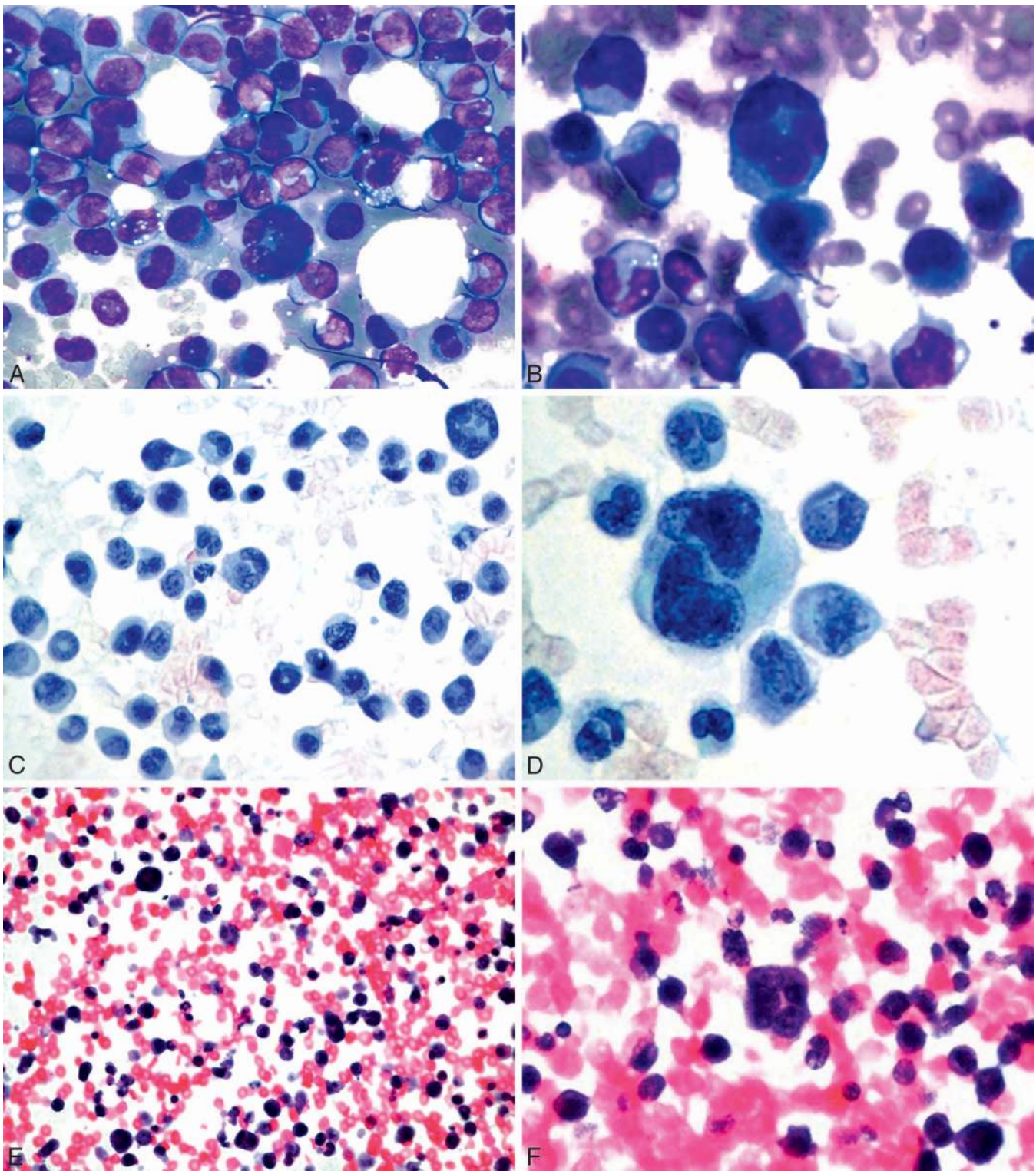

Figure 5. *Representative images of anaplastic T-cell lymphoma. A, Abundant lymphocytes with large atypical cells. B, The atypical cells with markedly enlarged "wreath cells." C and D, Some large, bilobed atypical pleomorphic cells. E and F, Cell block showing atypical multilobated giant cells that appear like "wreath cells" (Diff-Quik, original magnifications ×600 [A] and ×1000 [B]; Papanicolaou stain, original magnifications ×600 [C] and ×1000 [D]; hematoxylin-eosin, original magnifications ×400 [E] and ×1000 [F]).*

negative for CK and S100. This phenotype indicated the lymphoid nature of this tumor. Additional immunomarkers were applied, revealing tumor cells that were positive for CD4, CD30, epithelial membrane antigen, and anaplastic lymphoma kinase (ALK); rare for CD3 and CD2; and negative for CD20, CD10, CD5, and PAX-5. The MIB-1 was estimated at 80%. Representative images are shown in Figure 6. Flow cytometric studies were performed but were uninformative because of the lack of adequate viable cells.

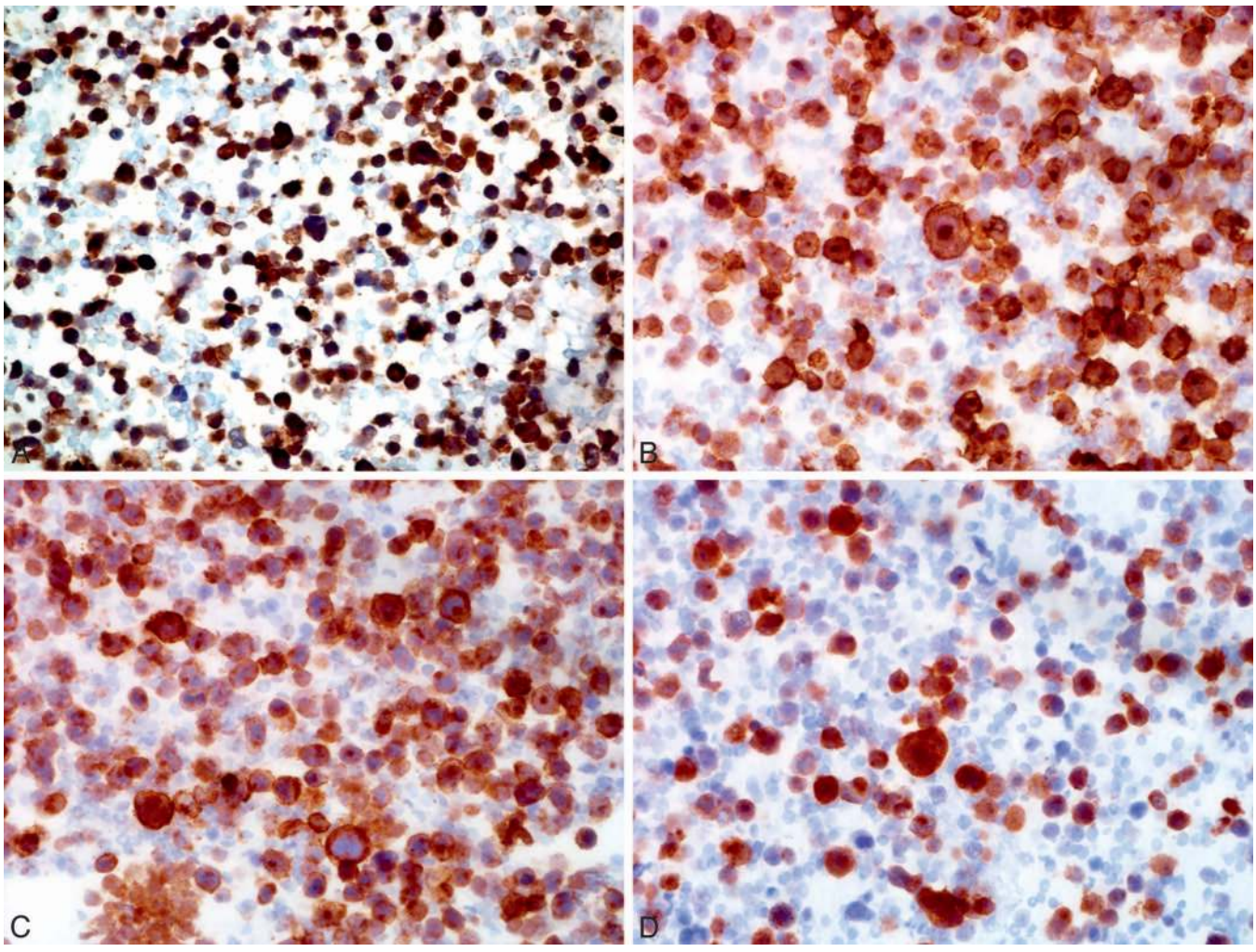

Figure 6. *Immunophenotype of anaplastic T-cell lymphoma. A, Leukocyte common antigen decorate both the large atypical cells as well as lymphocytes in the background. B, CD30⁺ tumor cells. C, CD4⁺ tumor cells. D, Anaplastic lymphoma kinase–positive tumor cells (original magnification ×600).*

These findings were consistent with ALK⁺ anaplastic T-cell lymphoma.

Anaplastic large cell lymphomas (ALCLs), initially described in 1985, are a subset of non-Hodgkin lymphomas that were previously called "Ki-1 lymphomas" and are characterized by large CD30⁺ (Ki-1⁺) anaplastic cells. The identification of the translocation of the chimeric fusion protein, a tyrosine kinase gene, *NPM-ALK*, involving *ALK* gene on chromosome 2p23 and the nucleophosmin (*NPM*) gene on chromosome 5q35, led to subsequent studies that revealed and subsequently confirmed that ALK⁺ ALCLs had a favorable prognosis.[36,37]

Peripheral T-cell lymphomas are not commonly seen, and ALCL is one of the most common subtypes, accounting for 25% of peripheral T-cell lymphomas in Western countries. The WHO classification currently recognizes 3 entities, including the ALK⁺ ALCL and ALK⁻ ALCL (a provisional entity in the WHO 2008 classification), which are systemic diseases, and the primary cutaneous ALCL.[38]

The cytologic features of ALK⁺ ALCL are quite variable; however, the characteristic cells known as "hallmark" or "wreath" cells are present in all cases. They are large cells with abundant cytoplasm, and the nuclei are often horseshoe- or donut-shaped or lobated. The hallmark cells can range from abundant to scant depending on the histologic variant.

The *WHO Classification of Tumours of Haematopoietic and Lymphoid Tissue*[36] describes several histologic variants, including the common variant, lymphohistiocytic variant, small cell variant, Hodgkin-like variant, and composite variant. The common type (described in the example above) shows sheets of large lymphoid cells featuring hallmark cells. The lymphohistiocytic variant accounts for 10% of ALK⁺ ALCLs and reveals abundant reactive histiocytes in addition to anaplastic tumor cells. The small cell variant accounts for 5% to 10% of ALCLs and is frequently considered a peripheral T-cell lymphoma. Both the lymphohistiocytic and small cell variants are more common in children and can often be misdiagnosed as benign infiltrates. The Hodgkin-like pattern (3%) may resemble nodular-sclerosing subtype of classical Hodgkin lymphoma with tumor nodules surrounded by fibrous bands. Immunohistochemically, ALK-positive ALCL expresses both CD30 and ALK, and the strong correlation between immunohistochemical positivity for ALK and the presence

of an ALK rearrangement has led to the use of immunohistochemistry to diagnose this entity.[39–46]

Anaplastic large cell lymphoma must be differentiated from other hematopoietic entities, like ALK$^+$ large B-cell lymphoma. The former is negative for CD20 and expresses CD30 (hallmark cells) in addition to ALK. ALK$^+$ large B-cell lymphomas are generally of immunoblastic/plasmablastic morphology, with large central nucleoli. They are typically negative for CD20 and CD30 immunostains and positive for CD138, epithelial membrane antigen, and ALK, and show light chain restriction with occasional multiple myeloma oncogene 1 (MUM1) positivity.

One must be aware of the pitfalls of ALK expression in other nonhematopoietic entities. *ALK* gene rearrangements and/or immunohistochemical expression is seen in lung adenocarcinomas, inflammatory myofibroblastic tumors, rhabdomyosarcomas, spindle cell/pleomorphic lipoma, intramuscular lipoma, Ewing sarcoma/peripheral primitive neuroectodermal tumors, malignant fibrous histiocytomas, and leiomyosarcomas.[44,46] MUM1, also called interferon regulatory factor 4 (IRF4), immunohistochemical staining is seen in a significant number of ALCLs that are ALK$^+$ (16 of 17; 94%) and ALK$^-$ (20 of 21; 91%).[47]

Melanoma

An 81-year-old man with prior history of squamous cell carcinoma of the skin presented with dizziness and difficulty breathing. A computed tomography image of the chest revealed multiple lung masses and lymphadenopathy. A possible brain lesion was also suspected because he complained of dizzy spells. The hilar lymph nodes were aspirated via endoscopic ultrasound guidance.

The smears were highly cellular, containing numerous single and loose clusters of spindled to plump cells with necrosis in the background. The atypical cells showed hyperchromatic nuclei without discernible nucleoli. Some rosettelike structures and scattered pigment-laden macrophages were evident. The cell block showed minute cores of tumor cells with spindled morphology, palisading around vessels. Representative images are shown in Figure 7, A through C.

The cellular findings, such as high cellularity with loosely cohesive and predominant single-cell pattern as well as the nuclear chromatin pattern, suggested a neuroendocrine neoplasm. However, the presence of dirty pigments in macrophages raised the possibility of a spindle cell melanoma. The palisading and rosettelike structures also brought neurogenic tumors, like malignant peripheral nerve sheath tumor (MPNST) and schwannoma, into the differential diagnosis considerations. The more frequently occurring sarcomatoid carcinoma was also considered.

A screening IHC panel to include CK, S100, synaptophysin, and vimentin was performed. The tumor cells were diffusely and strongly positive for S100 and vimentin, whereas CK and synaptophysin were negative. The profile strongly suggested a spindle cell melanoma or a neurogenic tumor, such as an MPNST, and, less likely, a schwannoma, given the presence of high-grade features. Additional immunohistochemical markers were applied and revealed tumor cell positivity for SOX10, Mart-1, and HMB-45. Representative images are illustrated in Figure 7, D through F.

The final diagnosis was consistent with metastatic melanoma, spindle cell morphology.

SOX10 is a member of the sex-determining region Y-related HMG-box family of transcription factors. This neural crest transcription factor is critical in the development and maintenance of Schwann cells and melanocytes, which allows for specific immunohistochemical characterization of tumors of melanocytic and Schwann cell lineage. The SOX10 protein is widely expressed in human benign tissues, including melanocytes, breast tissue, myoepithelial cells of salivary glands, cranial ganglia, dorsal root ganglia, and the otic vesicle. Therefore, it is also expressed in and identified on IHC in malignant tumors, such as melanoma, breast carcinoma, myoepithelioma, gliomas, and benign tumors, such as schwannomas.[48,49] Somatic mutations in the *SOX10* gene contribute to the development and progression of malignant melanoma and breast carcinoma.[50,51]

According to Nonaka et al,[52] SOX10 and S100 show nearly the same specificity and sensitivity for melanoma and neural tumors, such as schwannoma and neurofibroma. However , they show lower sensitivity for MPNST: only 49% (38 of 77) for SOX10 and 30% (23 of 77) for S100, as summarized in Table 6.

Several other studies[53–55] that investigated the staining pattern of SOX10 in melanocytic lesions showed 95% to 100% staining in conventional malignant melanomas, 100% staining in spindle cell melanomas and desmoplastic melanomas, and 97% to 100% staining in metastatic melanomas. Fortuitously, the entities that are usually considered in the differential diagnosis with MPNST, like the spindle cell monophasic synovial sarcomas, do not express SOX10.[56–58]

It seems imperative that a spindle cell lesion with SOX10 positivity be further worked up with melanocytic markers, like HMB-45 and Melan-A, to include or exclude melanocytic lesion. Benign and dysplastic nevi showed a 100% expression for SOX10; therefore, it is not useful in separating benign from malignant melanocytic proliferations. A small percentage (12%) of breast carcinomas (invasive ductal carcinomas and not lobular carcinomas) and all benign breast tissue (myoepithelial and lobular cells) were found to express SOX10.[52] In salivary gland tissues and tumors, SOX10 is a marker of acinus and intercalated duct differentiation. Acinic cell carcinomas, adenoid cystic carcinomas, epithelial-myoepithelial carcinomas, myoepithelial carcinomas, myoepitheliomas, and pleomorphic adenomas were reported to express SOX10.[59] Other tumors, such as ovarian (serous, clear, and poorly differentiated) carcinomas, endometrial (endometrioid and serous) carcinomas, lung (adenocarcinoma, squamous, poorly differentiated, and adenosquamous) carcinomas, and colon (well-differentiated and poorly differentiated) carcinomas showed no expression of SOX10.[60] Spindled fibroblasts and histiocytes, including epithelioid histiocytes as seen in scar tissue, showed weak to no staining with SOX10.[61]

Epithelioid Gastrointestinal Stromal Tumor

A 70-year-old woman from a mental health facility presented to the hospital with shortness of breath, altered mental status, and bone pain. The past medical records were fragmented; the caregiver had no relevant information except that she was diabetic and had a remote history of abdominal surgery. Imaging revealed multiple hepatic and pulmonary nodules and lymphadenopathy. An FNA of the mediastinal lymph node was performed under endoscopic ultrasound guidance.

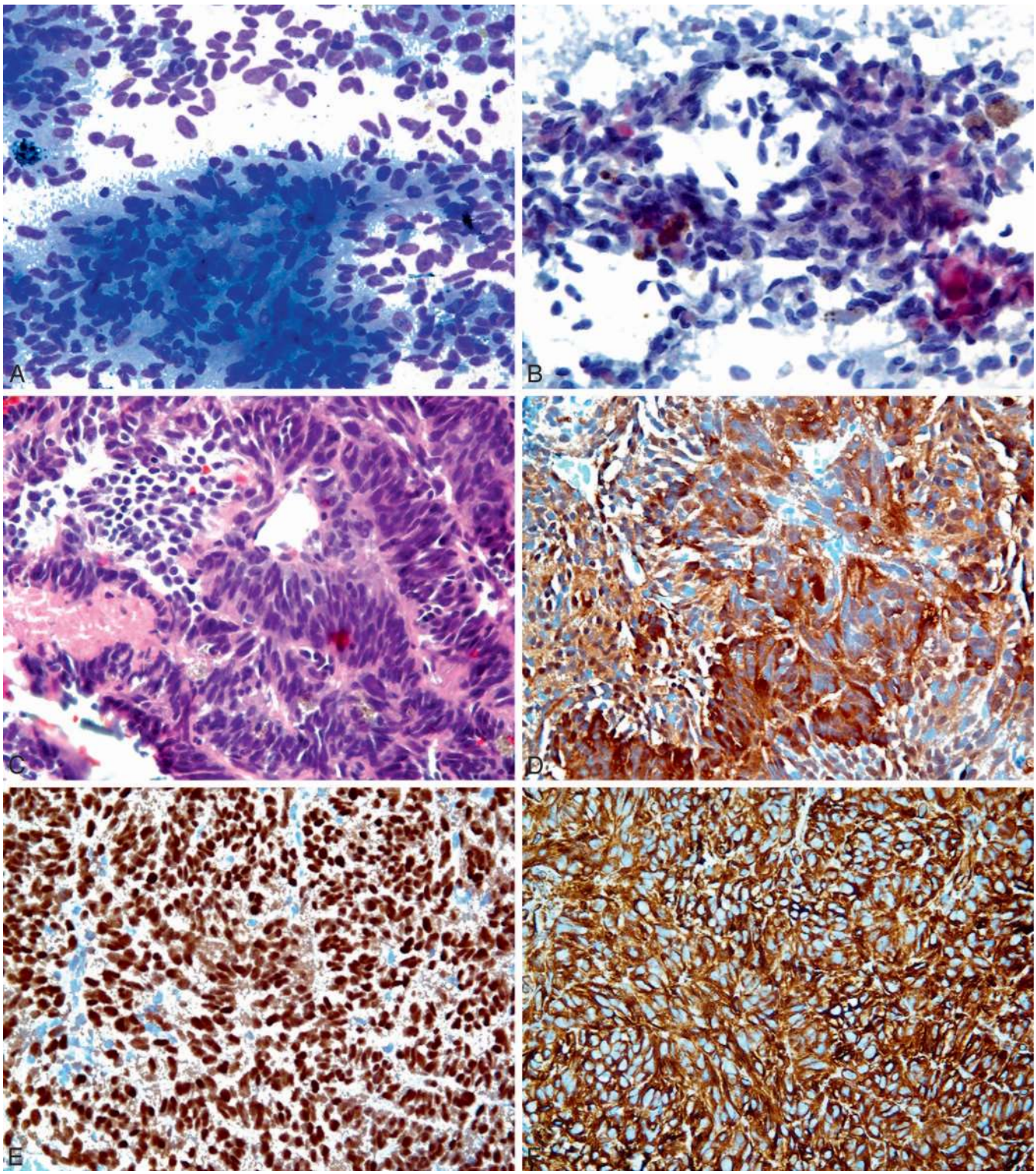

Figure 7. *Representative images of melanoma. A, Stain shows highly cellular smears with single and loose clusters of spindled to plump cells in a necrotic background. B, The tumor cells showing elongated nuclei without discernible nucleoli; in addition, dirty pigments in macrophages are demonstrated. C, The cell block showed cores of malignant spindle cells, with a focal palisading arrangement forming rosettelike structures, as well as focal areas of necrosis. D, S100 showing strong, diffuse nuclear and cytoplasmic staining. E, Nuclear staining for sex-determining region Y box 10 (SOX10). F, Tumor cells positive for vimentin (Diff-Quik, original magnification ×400 [A]; Papanicolaou stain, original magnification ×400 [B]; hematoxylin-eosin, original magnification ×400 [C]; original magnification ×400 [D through F]).*

Table 6. Sex-Determining Region Y Box 10 (SOX10) and S100 Staining in Malignant Melanoma and Neurogenic Tumors[a]

Tumors	SOX10, No. (%)	S100, No. (%)
Malignant melanoma		
Conventional	41/43 (95)	37/43 (86)
Spindle cell	7/7 (100)	7/7 (100)
Desmoplastic	28/28 (100)	27/28 (96)
Neurofibroma		
Cutaneous localized	12/12 (100)	12/12 (100)
Cutaneous diffuse	13/13 (100)	13/13 (100)
Plexiform	26/27 (96)	25/27 (93)
Schwannoma		
Conventional	26/26 (100)	26/26 (100)
Cellular	7/7 (100)	7/7 (100)
MPNST	38/77 (49)	23/77 (30)

Abbreviation: MPNST, malignant peripheral nerve sheath tumor.

[a] Data derived from Nonaka et al.[52]

The FNA smears were highly cellular, composed of large dyscohesive cells with round to oval, eccentrically located nuclei, discernible to prominent nucleoli, and moderate eosinophilic cytoplasm in a background of focal necrosis. There were occasional binucleated or multinucleated cells and rare intranuclear inclusions; few demonstrated rosetting and acini formation reminiscent of adenocarcinoma. The cell block revealed a few intact vascular, myxoid tissue fragments containing nests of spindled to plump cells showing similar morphology. Only rare mitotic figures were seen. Representative images are illustrated in Figure 8, A through C.

Based on the cytomorphology and histomorphology, the differential diagnosis generated included sarcomatoid carcinoma, melanoma, neuroendocrine neoplasm, plasmacytic neoplasm, and mesenchymal spindle cell tumors, including gastrointestinal stromal tumor (GIST) of the epithelioid subtype.

A screening panel of IHC consisting of CK, S100, LCA, synaptophysin, and vimentin was applied. It revealed tumor cells that were strongly positive for vimentin and negative for CK, S100, synaptophysin, and LCA. This phenotype led to a further workup to categorize this mesenchymal tumor. The additional IHC studies showed that the tumor cells were positive for CD117, discovered on GIST1 (DOG1), CD34, and smooth muscle actin stain, and negative for desmin. Representative images are illustrated in Figure 8, D through F.

The final diagnosis was consistent with GIST, epithelioid subtype.

Since the introduction of the term GIST by Mazur and Clark in 1983,[62] tremendous work at the subcellular and molecular levels has identified the interstitial cell of Cajal, the pacemaker cell responsible for controlling motility, to be the cell of origin for the GIST.[63] The discovery of c-kit proto-oncogene mutations in GISTs allowed for accurate segregation of GISTs from other mesenchymal lesions in the gastrointestinal tract.[64] CD117 (or c-kit), a transmembrane tyrosine kinase growth factor receptor involved in cellular differentiation, is expressed by the interstitial cells of Cajal, and therefore in most GISTs.

Morphologically, GISTs usually are spindle cell neoplasms composed of uniform spindle cells arranged in whorls or short intersecting fascicles. Nuclear palisading and extensive stromal hyalinization are also seen. An epithelioid morphology can also be seen, as shown in the index case above. Several other subtypes have been described.[65,66] Currently the prognosis of GIST is based on the size of tumor, mitotic count, and location of the tumor, as elucidated by Fletcher et al.[67]

About 80% of GISTs have c-kit mutations in the receptor tyrosine kinase (RTK) genes, which are positive for CD117 by immunohistochemistry. A small subset of GISTs, approximately 5% to 8%, has a platelet-derived growth factor receptor α (*PDGFRA*) mutation, which also causes activation of tyrosine kinase. This group of tumors is usually epithelioid in morphology, like in the example above. About 12% to 15% of GISTs lack the mutations for both genes and are known as wild-type GISTs. DOG1, a hypothetical protein encoded by gene *FLJ10261*, is a novel marker that is specifically expressed in GISTs expressing both the *c-kit* and *PDGFRA* mutations. The predominant staining pattern of DOG1 in epithelioid GIST is membranous, whereas it is membranous and cytoplasmic in spindle cell GIST.[68,69]

The importance of accurately identifying the presence of the mutation is critical because effective targeted therapies are now available and continue to be developed.[70,71] Although most GISTs are easily diagnosed based on clinical type, morphologic type, and immunophenotype, the small proportion of c-kit$^-$ (4%–15%)[69,70] GISTs will certainly benefit from identification by positive DOG1 staining, and thus further workup by screening for the mutations.

In the study by Espinosa et al,[72] DOG1 reactivity was seen in 370 GIST cases (87%), whereas the expression of KIT and CD34 on IHC was found in 317 cases (74%) and 254 cases (59%) of GISTs, respectively. These data suggest that the DOG1 antibody is more specific than c-kit because DOG1 can identify a small subset of c-kit$^-$ GISTs that may be amenable to kinase inhibitor therapy. The expression of DOG1, c-kit, and CD34 in GISTs with different mutations is summarized in Table 7.

DOG1 expression was relatively specific for GISTs among the mesenchymal tumors seen in the abdomen. In a study that included various mesenchymal and nonmesenchymal tumors, only rare cases of leiomyosarcoma (1 of 326; 0.3%), synovial sarcoma (1 of 39; 2.5%), and desmoplastic melanoma (1 of 10; 10%) were positive for DOG1. In contrast, CD117 expression was identified in 3 cases (0.9%) of leiomyosarcomas, 1 case (1.1%) of undifferentiated sarcomas, and occasional carcinomas of liver, pancreas, kidney, bladder, endometrial, and seminomas. Similar to DOG1, 1 case (10%) of desmoplastic melanoma was also reactive for CD117.[72] West et al[73] observed 4 cases (0.9%) of non-GIST tumors to be immunoreactive to DOG1 antiserum: 1 case (5%) of synovial sarcoma, 1 case (2.5%) of leiomyosarcoma, 1 case (25%) of fibrosarcoma, and 1 case (11%) of Ewing sarcoma/PNET.

Angiosarcoma

A 45-year-old morbidly obese man with a history of ulcerative colitis and type 2 diabetes presented with right upper quadrant pain. An ultrasound of the abdomen revealed a hepatic mass measuring 6.5 × 5.0 × 4.0 cm with adjacent fluid, suggesting hemorrhage. An ultrasound-guided FNA of the mass was performed.

The Diff-Quik–stained smear showed a few clusters of spindled to plump atypical cells with enlarged, hyperchromatic, and pleomorphic nuclei, some with prominent nucleoli in a bloody background. The cell block preparation

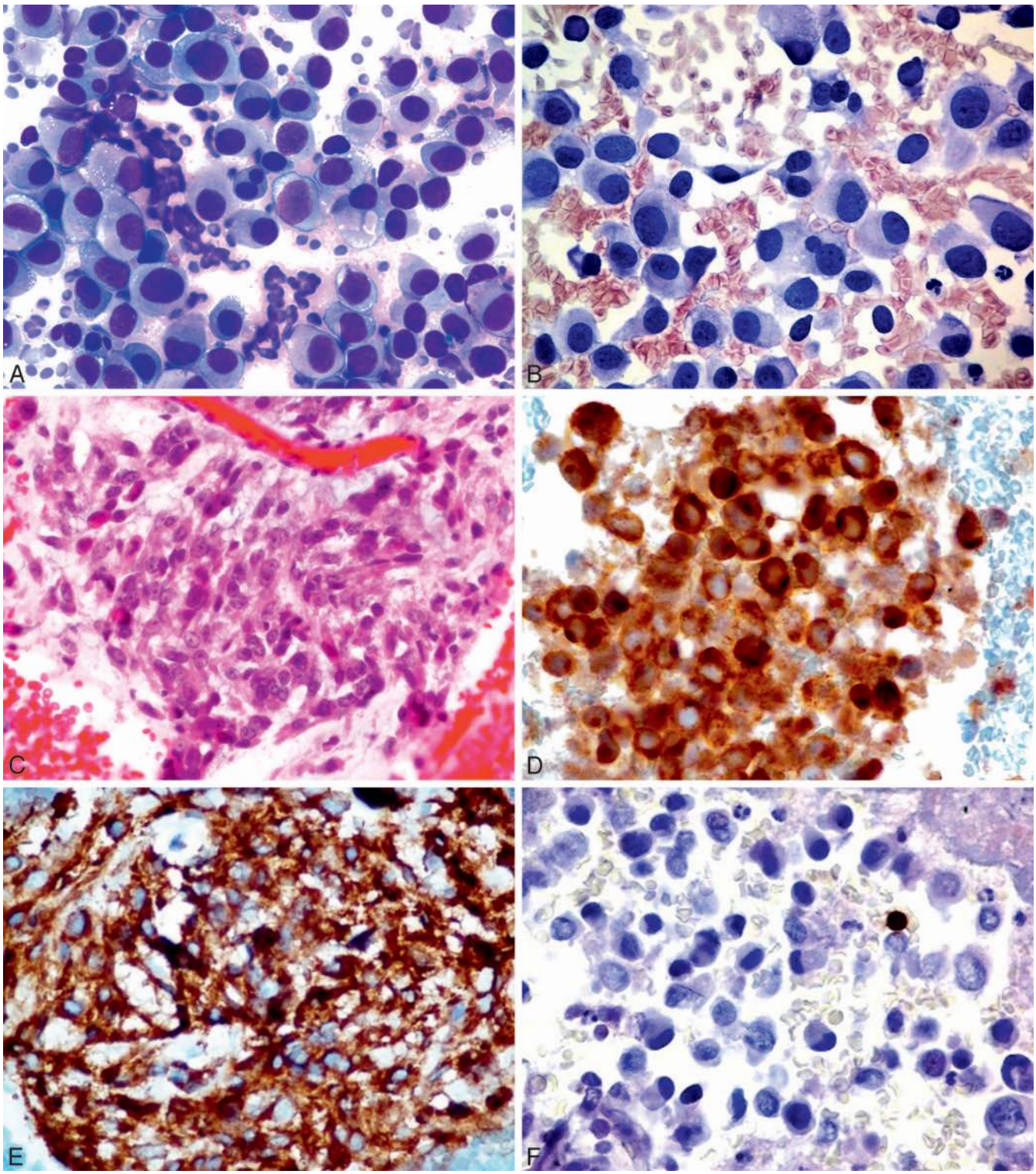

Figure 8. *Representative images of epithelioid gastrointestinal stromal tumor. A, Highly cellular smear composed of a population of large, dyscohesive, plasmacytoid cells. B, Round to oval nuclei with fine chromatin pattern and small nucleoli. C, The cell block section shows tissue fragments containing atypical cells in myxoid background. D, Tumor cells positive for CD117. E, Tumor cells positive for discovered on GIST1 (DOG1). F, Tumor cells negative for S100 (Diff-Quik, original magnification ×200 [A]; Papanicolaou stain, original magnification ×400 [B]; hematoxylin-eosin, original magnification ×600 [C]; original magnification ×600 [D through F]).*

Table 7. Comparison of Immunoreactivity of Discovered on GIST1 (DOG1) and c-kit in Wild-Type Gastrointestinal Stromal Tumors (GISTs) and GISTs With Mutations

Mutations	DOG1, No. (%)	c-kit (CD117), No. (%)
c-kit	200/218 (92)	180/221 (81)
PDGFRA	23/29 (79)	3/32 (9)
Wild-type GISTs	33/37 (89)	29/35 (83)
Total GISTs	370/425 (87)	317/428 (74)

Abbreviation: PDGFRA, platelet-derived growth factor receptor α.

revealed a minute tissue fragment composed of highly atypical spindled to plump cells with hyperchromatic and pleomorphic nuclei lining thin slitlike spaces with focal fibrinous material, as illustrated in Figure 9, A through C.

The cytomorphology and histomorphology suggest a spindle cell lesion. A screening panel of IHC to include CK, S100, vimentin, desmin, CD31, and CD34 was performed, revealing the tumor cells to be positive for vimentin, CD31, and CD34, and negative for CK, S100, and desmin. An ETS-related gene (ERG) immunostain highlighted the lining malignant cells, as illustrated in Figure 9, D.

The positive CD31, CD34, and ERG immunostaining confirmed the vascular origin of the tumor. The final diagnosis was consistent with angiosarcoma.

ERG immunostain, a member of the erythroblast transformation–specific (ETS) family of transcription factors, is responsible for regulating endothelial cell differentiation, angiogenesis, and expression of several endothelial-specific antigens.[74–76] ERG overexpression was first described in prostatic adenocarcinomas resulting from the transmembrane protease serine 2 (*TMPRSS2*)-*ERG* oncogene translocations.[77–79]

Our previous study[80] on ERG expression by IHC evaluation in prostrate carcinoma, high-grade prostatic intraepithelial neoplasia, and other benign conditions revealed that overexpression of ERG is specific for prostate carcinoma, albeit with a relatively low sensitivity. Only 44% (40 of 90) of low-grade prostatic adenocarcinomas (Gleason scores 3 + 3 or 3 + 4) and 22% (8 of 36) of high-grade prostatic adenocarcinomas (Gleason scores 4 + 4 or above) showed staining with ERG immunostain. Premalignant lesions, such as high-grade prostatic intraepithelial neopla-

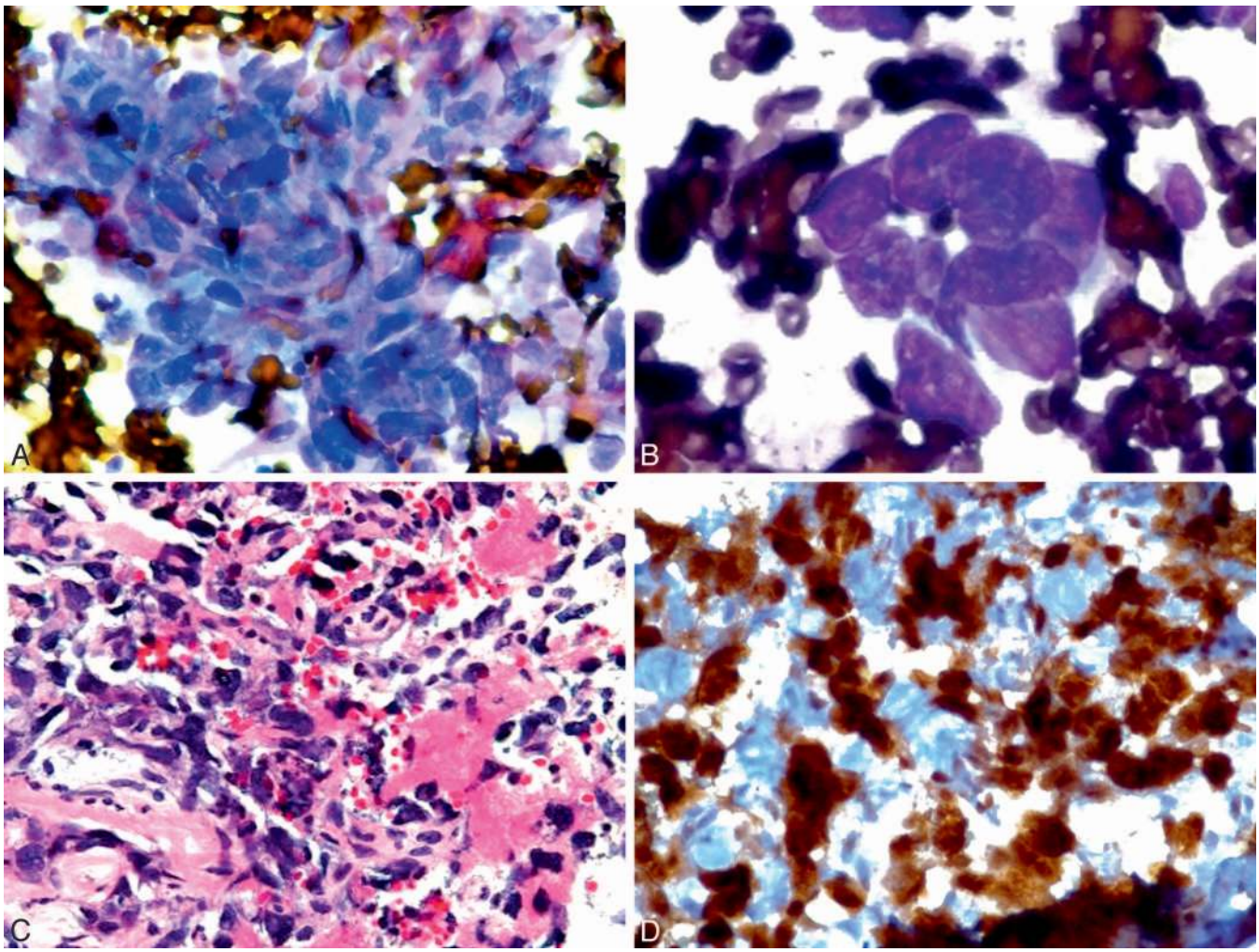

Figure 9. *Representative images of angiosarcoma. A and B, Clusters of spindled to plump atypical cells with enlarged, hyperchromatic nuclei with conspicuous nucleoli. C, The tissue fragment in the cell block shows atypical spindle cells with hyperchromatic nuclei lining thin slitlike spaces; in addition, fibrin deposits are noted. D, The tumor cells were positive for ETS-related gene protein (ERG) (Diff-Quik, original magnification ×600 [A and B]; hematoxylin-eosin, original magnification ×600 [C]; original magnification ×600 [D]).*

sia, showed a positive rate of 22% (4 of 18). Of the 4 cases that were positive, 3 were associated with prostatic adenocarcinoma, and the other was associated with atypical small acinar proliferation. Benign conditions, like radiation atypia (n = 20) and atrophic glands (n = 18), showed no reactivity to ERG staining. Normal prostatic tissue and seminal vesicles were also nonreactive. A large series of nonprostate carcinomas/neoplasms were nonreactive as well.

Other studies have found that ERG is an immunohistochemical marker for vascular tumors, including lymphangiomas and hemangiomas of various subtypes, and is seen in a nuclear staining pattern. In addition, 7 cases (70%) of blastic extramedullary myeloid tumors (acute myeloid leukemia tissue infiltrates) and 2 cases (7%) of Ewing sarcomas expressed ERG, likely secondary to the TLS/FUS-ERG fusion transcripts and Ewing sarcoma breakpoint region 1 *(EWSR1)-ERG* rearrangement, respectively. Other nonvascular and nonepithelial tumors, such as mesenchymal, neuroectodermal, and hematopoietic tumors, were nonreactive to ERG.[81]

ERG was expressed in 41 cases (38%) of epithelioid sarcomas, usually with a uniform nuclear staining similar to that seen in angiosarcomas, whereas other endothelial markers, like CD31, were negative. However, all epithelioid sarcomas were negative for *ERG* gene rearrangement, indicating that ERG expression in epithelioid sarcoma is not likely related to *ERG*-involved translocations.[82]

The lack of ERG reactivity in adenocarcinomas of the breast, colon, lung, stomach, and epithelial malignancies that frequently metastasize proves ERG to be a suitable marker of possible prostatic origin.[83]

Dysgerminoma

A 23-year-old woman with no significant past medical history presented with lower abdominal discomfort. Imaging revealed a large retroperitoneal mass and an enlarged periaortic lymph node measuring 3 cm. An FNA of the lymph node was performed.

The smears revealed few clusters of pleomorphic cells containing prominent nucleoli and abundant cytoplasm admixed with scattered lymphocytes. The background showed a tiger-stripe pattern, as illustrated in Figure 10, A. The cell block preparation revealed rare tissue fragments containing foci of hyperchromatic, large polygonal cells with intermingled lymphocytes as well as focal tumor necrosis, as illustrated in Figure 10, B. The cytologic findings, such as large polygonal cells with centrally placed pleomorphic nuclei and admixed with lymphocytes in the tiger-stripe background, were suggestive of a germ cell tumor (GCT)—that is, dysgerminoma.

An IHC screening panel to include CK, LCA, S100, and vimentin, as well as germ cell markers (ie, Sal-like protein 4 [SALL4], octamer-binding transcription factor 3/4 [OCT3/4], NANOG, and CD117), was performed. The tumor cells were positive for CK, SALL4, OCT3/4, NANOG, and CD117, and negative for LCA, S100, and vimentin, as illustrated in Figure 10, C through F.

These findings are consistent with metastatic dysgerminoma.

Germ cell tumors account for greater than 95% of testicular neoplasms and less than 1% of ovarian malignancies. The distinction of seminomatous from nonseminomatous GCTs is critical for management and predicting prognostic outcomes. However, this distinction can be challenging in cytology specimens, given the paucity of diagnostic material and the lack of histomorphology. In the setting of lymph node metastasis, the lack of the history of a GCT adds another level of complexity to the diagnosis on a scant FNA specimen. Picking up on subtle cytologic clues, such as tiger-stripe background and biphasic population of cells, plays a key role in initiating the workup for GCTs.

The newer embryonic stem cell transcription factors, OCT3/4 (OCT4), NANOG, and SOX2, play an important role in stem cell growth and differentiation. Immunohistochemically, different expression patterns were noted in various subtypes of GCTs, like seminoma, embryonal carcinoma, yolk sac tumor, teratoma and choriocarcinoma, in primary and metastatic lesions.

The study by Santagata et al[84] including 21 cases of pure primary testicular GCTs (14 seminoma, 3 embryonal carcinoma, and 4 teratoma), 20 cases of mixed GCTs (foci of 15 embryonal carcinoma, 6 seminoma, 15 teratoma, 6 yolk sac tumor, and 5 choriocarcinoma), and 43 cases of retroperitoneal metastatic GCTs (with components of 8 seminoma, 21 embryonal carcinoma, 16 teratoma, 6 yolk sac tumor, and 2 choriocarcinoma) reported the expression of NANOG and OCT3/4 in both primary and metastatic seminomas as well as in embryonal carcinoma. However, these immunomarkers were negative in yolk sac tumors and choriocarcinomas. The immunomarker SOX2 was positive for embryonal carcinoma but negative in seminomas, yolk sac tumors, and choriocarcinomas. The study results are summarized in Table 8.

A study performed at our institution[85] confirmed NANOG expression in 17 cases (100%) of testicular intraepithelial germ cell neoplasm, 23 cases (96%) of testicular classic seminomas, and 16 cases (94%) of testicular embryonal carcinomas. It was observed that none of the testicular yolk sac tumors or other testicular tumors, such as spermatocytic seminoma and Leydig cell tumor, stained positively. Other epithelial neoplasms, including urothelial carcinoma (n = 31), RCC (n = 46), hepatocellular carcinoma and cholangiocarcinomas (n = 22), gastrointestinal adenocarcinoma (n = 64), gynecologic (uterine and ovarian) carcinomas (n = 66), prostate adenocarcinoma (n = 124), lung carcinoma (small and non–small cell carcinoma; n = 206), pancreatic adenocarcinoma (n = 60), breast carcinoma (n = 171), and thyroid carcinoma (n = 72), were all nonreactive for NANOG.

In other studies performed at our institution (F.L., unpublished data, March 2012), SOX2 expression in 1020 cases of tumors from various organs revealed positive SOX2 staining in 16 cases (63%) of embryonal carcinomas and 7 cases (57%) of yolk sac tumors, whereas no staining was observed in the seminomas (n = 21). In a study comparing the IHC patterns of placental alkaline phosphatase and NANOG in identifying central nervous system germinomas,[86] NANOG was found to be a better marker than placental alkaline phosphatase because of its strong nuclear signal. Placental alkaline phosphatase, a reasonably sensitive diagnostic marker for GCTs, often showed weak and patchy cytoplasmic staining, and therefore was considered less reliable. Other central nervous system tumors, such as pineoblastomas, medulloblastomas, high-grade gliomas, pituitary adenomas, supratentorial primitive neuroectodermal tumors, central neurocytomas, Langerhans cell histiocytosis, atypical teratoid/rhabdoid tumors, and non-Hodgkin lymphomas, were all negative for NANOG.

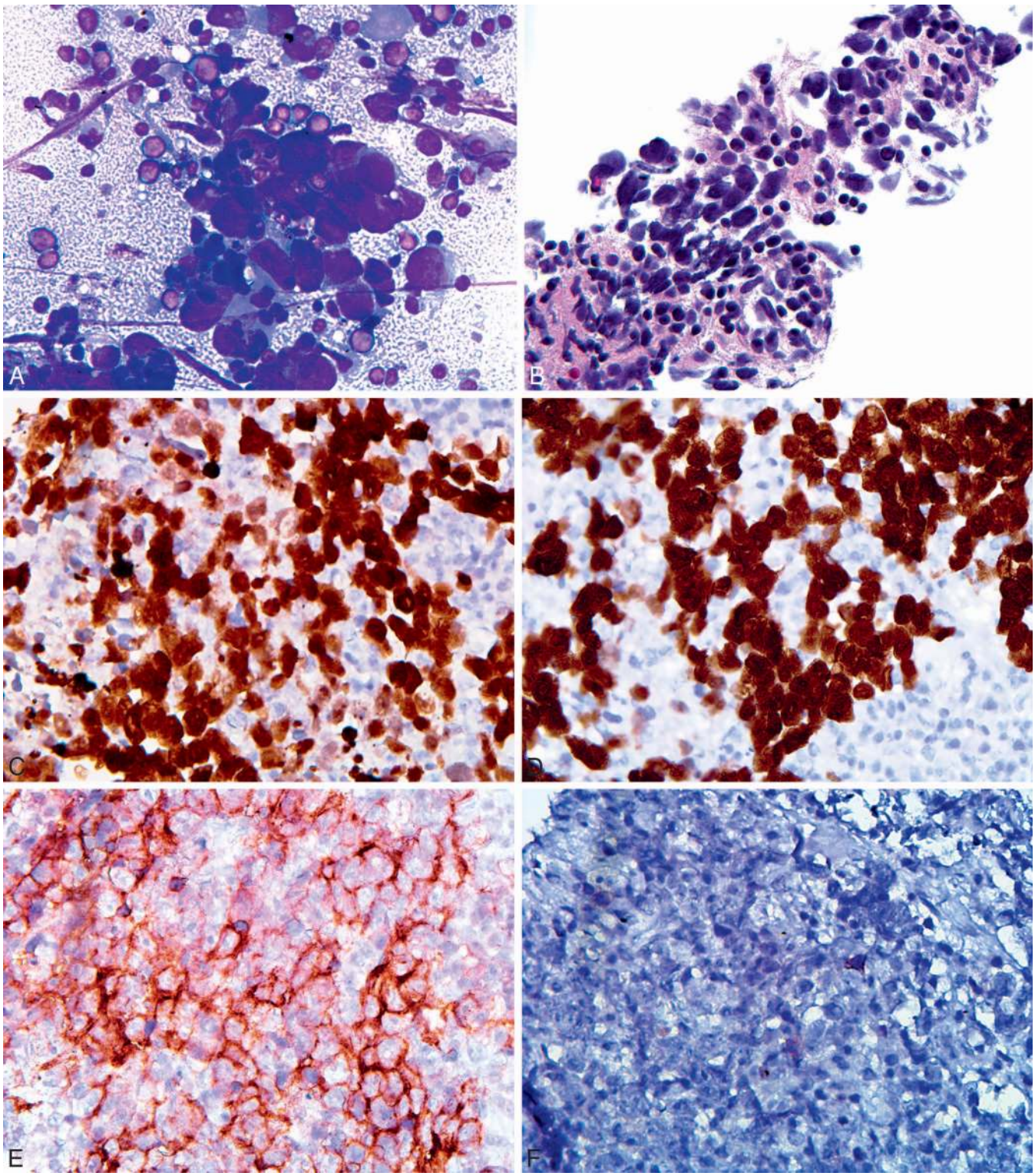

Figure 10. *Representative images of dysgerminoma. A, A few cohesive clusters of large polygonal tumor cells with pleomorphic nuclei containing prominent nucleoli and abundant vacuolated cytoplasm admixed with lymphocytes; also noted is the diagnostic "tiger-stripe" pattern in the background. B, The cell block section showed tissue cores with a small cluster of atypical cells with hyperchromatic, irregular nuclei interspersed with lymphocytes. C, Nuclear staining for NANOG. D, Nuclear staining for Sal-like protein 4 (SALL4). E, Positive for CD117. F, Negative for CD30 (Diff-Quik, original magnification ×600 [A]; hematoxylin-eosin, original magnification ×200 [B]; original magnification ×400 [C through F]).*

Although negative results for NANOG in breast carcinomas (n = 171) have been seen in our experience, expression of NANOG protein was found in an unknown number of samples of the Michigan Cancer Foundation-7 (MCF-7) breast carcinoma cell line.[87] This study found that NANOG was expressed in breast carcinoma but not in normal breast tissue, and this should be a potential pitfall of which one must be aware.

Table 8. Immunostaining Pattern of Testicular Germ Cell Tumors

Tumors	NANOG	OCT3/4	SOX2
Seminoma	+	+	−
Embryonal carcinoma	+	+	+
Yolk sac tumor	−	−	−
Choriocarcinoma	−	−	−

Abbreviations: OCT3/4, octamer-binding transcription factor 3/4; SOX2, sex-determining region Y box 2.

CONCLUSIONS

In the era of expanding knowledge on tumor genomics with accompanied targeted therapy, the role of cytopathologists is expanding. Lending an accurate diagnosis to each specimen is only a part of the service provided to patients. The preservation of limited diagnostic material for potential molecular and other ancillary testing, as well as the selection of those assays, is critical, and these are some of the newer responsibilities of the "guardians of the tissue." A systematic approach along every step of the process, beginning with rapid on-site evaluation and including the cytomorphologic or histomorphologic evaluation, the algorithmic application of a small and effective panel of immunomarkers, and the precise selection of molecular or other ancillary tests, is required. This allows for the most efficient use of the limited material available on the cell block, and hence allows for better patient care.

Through this paper we have emphasized the key role of cytopathology or histomorphology in generating appropriate differential diagnoses and ultimately arriving at an accurate diagnosis. An algorithmic approach to working up tumors of unknown primary origin and effective small panels of IHC were proposed, and discussions of the potential pitfalls were elaborated. The application of the algorithms and IHC panels was illustrated through 7 selected presentations, which were entities commonly seen in tumors of unknown primary origin. The small screening panel consisting of CK, S100, vimentin, and LCA allows for lineage specification and provides a direction for further workup. The organ- or tumor-specific immunomarkers, including some newer generations of immunomarkers, help to achieve a specific diagnosis. By exercising a systematic approach for working up tumors of unknown primary origin, not only can an accurate specific diagnosis be reached, but also the preservation of tissue for potential molecular or other ancillary testing can be achieved in most cases of daily practice.

References

1. Lin F, Liu H. Unknown primary/undifferentiated neoplasms in surgical and cytologic specimens. In: Lin F, Prichard JW, Liu H, Wilkerson M, Schuerch C, eds. *Handbook of Practical Immunohistochemistry: Frequently Asked Questions*. New York, NY: Springer; 2011:55–83.
2. Chu P, Wu E, Weiss LM. Cytokeratin 7 and cytokeratin 20 expression in epithelial neoplasms: a survey of 435 cases. *Mod Pathol*. 2000;13(9):962–972.
3. Lin F, Liu H. Immunohistochemistry in undifferentiated neoplasm/tumor of uncertain origin. *Arch Pathol Lab Med*. 2014;138(12):1583–1610.
4. Ordóñez NG. Broad-spectrum immunohistochemical epithelial markers: a review. *Hum Pathol*. 2013;44(7):1195–1215.
5. Gaffey MJ, Traweek ST, Mills SE, et al. Cytokeratin expression in adrenocortical neoplasia: an immunohistochemical and biochemical study with implications for the differential diagnosis of adrenocortical, hepatocellular, and renal cell carcinoma. *Hum Pathol*. 1992;23(2):144–153.
6. Cote RJ, Cordon-Cardo C, Reuter VE, Rosen PP. Immunopathology of adrenal and renal cortical tumors: coordinated change in antigen expression is associated with neoplastic conversion in the adrenal cortex. *Am J Pathol*. 1990; 136(5):1077–1084.
7. Michels S, Swanson PE, Frizzera G, Wick MR. Immunostaining for leukocyte common antigen using an amplified avidin-biotin-peroxidase complex method and paraffin sections: a study of 735 hematopoietic and nonhematopoietic human neoplasms. *Arch Pathol Lab Med*. 1987;111(11):1035–1039.
8. Kurtin PJ, Pinkus GS. Leukocyte common antigen–a diagnostic discriminant between hematopoietic and nonhematopoietic neoplasms in paraffin sections using monoclonal antibodies: correlation with immunologic studies and ultrastructural localization. *Hum Pathol*. 1985;16(4):353–365.
9. Kahwash SB, Qualman SJ. Cutaneous lymphoblastic lymphoma in children: report of six cases with precursor B-cell lineage. *Pediatr Dev Pathol*. 2002;5(1):45–53.
10. Ozdemirli M, Fanburg-Smith JC, Hartmann DP, Azumi N, Miettinen M. Differentiating lymphoblastic lymphoma and Ewing's sarcoma: lymphocyte markers and gene rearrangement. *Mod Pathol*. 2001;14(11):1175–1182.
11. Nandedkar MA, Palazzo J, Abbondanzo SL, Lasota J, Miettinen M. CD45 (leukocyte common antigen) immunoreactivity in metastatic undifferentiated and neuroendocrine carcinoma: a potential diagnostic pitfall. *Mod Pathol*. 1998; 11(12):1204–1210.
12. Herrera GA, Turbat-Herrera EA, Lott RL. S-100 protein expression by primary and metastatic adenocarcinomas. *Am J Clin Pathol*. 1988;89(2):168–176.
13. Bahrami A., Truong LD, Ro JY. Undifferentiated tumor: true identity by immunohistochemistry. *Arch Pathol Lab Med*. 2008;132(3):326–348.
14. Shuch B, Amin A, Armstrong AJ, et al. Understanding pathologic variants of renal cell carcinoma: distilling therapeutic opportunities from biologic complexity. *Eur Urol*. 2015;67(1):85–97.
15. Grignon DJ, Eble JN. Papillary and metanephric adenomas of the kidney. *Semin Diagn Pathol*. 1998;15(1):41–53.
16. Delahunt B, Eble JN. Papillary renal cell carcinoma: a clinicopathologic and immunohistochemical study of 105 tumors. *Mod Pathol*. 1997;10(6):537–544.
17. Chu PG, Weiss LM. *Modern Immunohistochemistry*. New York, NY: Cambridge University Press; 2009.
18. Klatte T, Pantuck AJ, Said JW, et al. Cytogenetic and molecular tumor profiling for type 1 and type 2 papillary renal cell carcinoma. *Clin Cancer Res*. 2009;15(4):1162–1169.
19. Waldert M, Haitel A, Marberger M, et al. Comparison of type I and II papillary renal cell carcinoma (RCC) and clear cell RCC. *BJU Int*. 2008;102(10): 1381–1384.
20. Furge KA, Chen J, Koeman J, et al. Detection of DNA copy number changes and oncogenic signaling abnormalities from gene expression data reveals MYC activation in high-grade papillary renal cell carcinoma. *Cancer Res*. 2007;67(7):3171–3176.
21. Schmidt L, Duh FM, Chen F, et al. Germline and somatic mutations in the tyrosine kinase domain of the MET proto-oncogene in papillary renal carcinomas. *Nat Genet*. 1997;16(1):68–73.
22. Martin B, Poblet E, Rios JJ, et al. Merkel cell carcinoma with divergent differentiation: histopathological and immunohistochemical study of 15 cases with PCR analysis for Merkel cell polyomavirus. *Histopathology*. 2013;62(5): 711–722.
23. Bobos M, Hytiroglou P, Kostopoulos I, Karkavelas G, Papadimitriou CS. Immunohistochemical distinction between Merkel cell carcinoma and small cell carcinoma of the lung. *Am J Dermatopathol*. 2006;28(2):99–104.
24. Leech SN, Kolar AJ, Barrett PD, Sinclair SA, Leonard N. Merkel cell carcinoma can be distinguished from metastatic small cell carcinoma using antibodies to cytokeratin 20 and thyroid transcription factor 1. *J Clin Pathol*. 2001; 54(9):727–729.
25. Ralston J, Chiriboga L, Nonaka D. MASH1: a useful marker in differentiating pulmonary small cell carcinoma from Merkel cell carcinoma. *Mod Pathol*. 2008;21(11):1357–1362.
26. Feng H, Shuda M, Chang Y, Moore PS. Clonal integration of a polyomavirus in human Merkel cell carcinoma. *Science*. 2008;319(866): 1096–1100.
27. Andres C, Belloni B, Puchta U, Sander CA, Flaig MJ. Re: clinical factors associated with Merkel cell polyomavirus infection in Merkel cell carcinoma. *J Natl Cancer Inst*. 2009;101(23):1655–1656.
28. Sihto H, Kukko H, Koljonen V, Sankila R, Bohling T, Joensuu H. Clinical factors associated with Merkel cell polyomavirus infection in Merkel cell carcinoma. *J Natl Cancer Inst*. 2009;101(13): 938–945.
29. Ashman LK. The biology of stem cell factor and its receptor C-kit. *Int J Biochem Cell Biol*. 1999;31(10):1037–1051.
30. Su LD, Fullen DR, Lowe L, Uherova P, Schnitzer B, Valdez R. CD117 (KIT receptor) expression in Merkel cell carcinoma. *Am J Dermatopathol*. 2002;24(4): 289–293.
31. Rio MC. From a unique cell to metastasis is a long way to go: clues to stromelysin-3 participation. *Biochimie*. 2005;87(3–4):299–306.
32. Turdean SG, Gurzu S, Jung I, Neagoe RM, Sala D. Unexpected maspin immunoreactivity in Merkel cell carcinoma. *Diagn Pathol*. 2015;10:206.
33. Iliadis A, Koletsa T, Kostopoulos I, Tzioufa V. Letter to the editor: diffuse TTF-1 expression in a case of Merkel cell carcinoma. *Pol J Pathol*. 2015;66(2): 200–201.
34. Kolhe R, Reid MD, Lee JR, Cohen C, Ramalingam P. Immunohistochemical expression of PAX5 and TdT by Merkel cell carcinoma and pulmonary small cell carcinoma: a potential diagnostic pitfall but useful discriminatory marker. *Int J Clin Exp Pathol*. 2013;6(2):142–147.

35. Visscher D, Cooper PH, Zarbo RJ, Crissman JD. Cutaneous neuroendocrine (Merkel cell) carcinoma: an immunophenotypic, clinicopathologic, and flow cytometric study. *Mod Pathol*. 1989;2(4):331–338.
36. Swerdlow SH, Campo E, Harris NL, et al. *WHO Classification of Tumours of Haematopoietic and Lymphoid Tissue*. 4th ed. Lyon, France: IARC Press; 2008. *World Health Organization Classification of Tumours*; vol. 2.
37. Stein H, Foss HD, Dürkop H, et al. CD30(+) anaplastic large cell lymphoma: a review of its histopathologic, genetic, and clinical features. *Blood*. 2000;96(12):3681–3695.
38. Laharanne E, Oumouhou N, Bonnet F, et al. Genome-wide analysis of cutaneous T-cell lymphomas identifies three clinically relevant classes. *J Invest Dermatol*. 2010;130(6):1707–1718.
39. Savage KJ, Harris NL, Vose JM, et al. ALK- anaplastic large cell lymphoma is clinically and immunophenotypically different from both ALK+ ALCL and peripheral T-cell lymphoma, not otherwise specified: report from the International Peripheral T-Cell Lymphoma Project. *Blood*. 2008;111(12):5496–5504.
40. Savage KJ, Chhanabhai M, Gascoyne RD, Connors JM. Characterization of peripheral T-cell lymphomas in a single North American institution by the WHO classification. *Ann Oncol*. 2004;15(10):1467–1475.
41. Vose J, Armitage J, Weisenburger D; International T-Cell Lymphoma Project. International peripheral T-cell and natural killer/T-cell lymphoma study: pathology findings and clinical outcomes. *J Clin Oncol*. 2008;26(25):4124–4130.
42. Rizvi MA, Evens AM, Tallman MS, Nelson BP, Rose ST. T-cell non-Hodgkin lymphoma. *Blood*. 2006;107(4):1255–1264.
43. Falini B, Pileri S, Zinzani PL, et al. ALK+ lymphoma: clinic-pathological findings and outcome. *Blood*. 1999;93(8):2697–2706.
44. Xing X, Feldman AL. Anaplastic large cell lymphomas: ALK positive, ALK negative, and primary cutaneous. *Adv Anat Pathol*. 2015;22(1):29–49.
45. Willemze R, Beljaards RC. Spectrum of primary cutaneous CD30 (Ki-1)-positive lymphoproliferative disorders: a proposal for classification and guidelines for management and treatment. *J Am Acad Dermatol*. 1993;28(6):973–980.
46. Li XQ, Hisaoka M, Shi DR, Zhu XZ, Hashimoto H. Expression of anaplastic lymphoma kinase in soft tissue tumors: an immunohistochemical and molecular study of 249 cases. *Hum Pathol*. 2004:35(6):711–721.
47. Feldman AL, Law M, Remstein ED, et al. Recurrent translocations involving the IRF4 oncogene locus in peripheral T-cell lymphomas. *Leukemia*. 2009;23(3):574–580.
48. Harris ML, Baxter LL, Loftus SK, Pavan WJ. Sox proteins in melanocyte development and melanoma. *Pigment Cell Melanoma Res*. 2010;23(4):496–513.
49. Cook AL, Smith AG, Smit DJ, LeonardJH, Sturm RA. Co-expression of SOX9 and SOX10 during melanocytic differentiation in vitro. *Exp Cell Res*. 2005;308(1):222–235.
50. Yang GG, Minasyan A, Gordon J, et al. Rabbit polyclonal anti-SOX10 is a reliable IHC marker for melanoma and its mimics [USCAP Abstract 514]. *Mod Pathol*. 2013;26(suppl S2):124A–125A.
51. Kang Y, Pekmezci M, Scheithauer B, et al. Utility of Sox-10 to distinguish MPNST from synovial sarcoma with a focus on intraneural synovial sarcoma [USCAP Abstract 56]. *Mod Pathol*. 2013;26(suppl S2):14A.
52. Nonaka D, Chiriboga L, Rubin BP. Sox10: a pan-schwannian and melanocytic marker. *Am J Surg Pathol*. 2008;32(9):1291–1298.
53. Ramos-Herberth FI, Karamchandani J, Dadras SS. SOX10 immunostaining distinguishes desmoplastic melanoma from excision scar. *J Cutan Pathol*. 2010;37(9):944–952.
54. Ordóñez NG, Mahfouz SM, Mackay B. Synovial sarcoma: an immunohistochemical and ultrastructural study. *Hum Pathol*. 1990;21(7):733–749.
55. Krane JF, Bertoni F, Fletcher CD. Myxoid synovial sarcoma: an underappreciated morphologic subset. *Mod Pathol*. 1999;12(5):456–462.
56. Smith TA, Machen SK, Fisher C, Goldblum JR. Usefulness of cytokeratin subsets for distinguishing monophasic synovial sarcoma from malignant peripheral nerve sheath tumor. *Am J Clin Pathol*. 1999;112(5):641–648.
57. Pelmus M, Guillou L, Hostein I, et al. Monophasic fibrous and poorly differentiated synovial sarcoma: immunohistochemical reassessment of 60 t(X;18)(SYT-SSX)-positive cases. *Am J Surg Pathol*. 2002;26(11):1434–1440.
58. Karamchandani JR, Nielsen TO, van de Rijn M, West RB. Sox10 and S100 in the diagnosis of soft-tissue neoplasms. *Appl Immunohistochem Mol Morphol*. 2012;20(5):445–450.
59. Ohtomo R, Mori T, Shibata S, et al. SOX10 is a novel marker of acinus and intercalated duct differentiation in salivary gland tumors: a clue to the histogenesis for tumor diagnosis. *Mod Pathol*. 2013;26(8):1041–1450.
60. Mohamed A, Gonzalez RS, Lawson D, Wang J, Cohen C. SOX10 expression in malignant melanoma, carcinoma, and normal tissues. *Appl Immunohistochem Mol Morphol*. 2013;21(6):506–510.
61. Ohsie SJ, Sarantopoulos GP, Cochran AJ, Binder SW. Immunohistochemical characteristics of melanoma. *J Cutan Pathol*. 2008;35(5):433–444.
62. Mazur MT, Clark HB. Gastric stromal tumors: reappraisal of histogenesis. *Am J Surg Pathol*. 1983;7(6):507–519.
63. Kindblom LG, Remotti HE, Aldenborg F, Meis-Kindblom JM. Gastrointestinal pacemaker cell tumor (GIPACT): gastrointestinal stromal tumors show phenotypic characteristics of the interstitial cells of Cajal. *Am J Pathol*. 1998;152(5):1259–1269.
64. Hirota S, Isozaki K, Moriyama Y, et al. Gain-of-function mutations of c-kit in human gastrointestinal stromal tumors. *Science*. 1998;279(5350):577–580.
65. Berman J, O'Leary TJ. Gastrointestinal stromal tumour workshop. *Hum Pathol*. 2001;32(6):578–582.
66. Miettinen M, Sobin LH, Lasota J. Gastrointestinal stromal tumors of the stomach: a clinicopathologic, immunohistochemical, and molecular genetic study of 1765 cases with long-term follow-up. *Am J Surg Pathol*. 2005;29(1):52–68.
67. Fletcher C, Berman J, Corless C, et al. Diagnosis of gastrointestinal stromal tumors: a consensus approach. *Hum Pathol*. 2002;33(5):459–465.
68. Hirota S, Ohashi A, Nishida T, et al. Gain-of-function mutations of platelet-derived growth factor receptor alpha gene in gastrointestinal stromal tumors. *Gastroenterology*. 2003;125(3):660–667.
69. Heinrich MC, Corless CL, Duensing A, et al. PDGFRA activating mutations in gastrointestinal stromal tumours. *Science*. 2003;299(5607):708–710.
70. Demetri GD, von Mehren M, Blanke CD, et al. Efficacy and safety of imatinib mesylate in advanced gastrointestinal stromal tumors. *N Engl J Med*. 2002;347(7):472–480.
71. Sarlomo-Rikala M, Kovatich AJ, Barusevicius A, Miettinen M. CD117: a sensitive marker for gastrointestinal stromal tumors that is more specific than CD34. *Mod Pathol*. 1998;11(8):728–734.
72. Espinosa I, Lee CH, Kim MK, et al. A novel monoclonal antibody against DOG1 is a sensitive and specific marker for gastrointestinal stromal tumors. *Am J Surg Pathol*. 2008;32(2):210–218.
73. West RB, Corless CL, Chen X, et al. The novel marker, DOG1, is expressed ubiquitously in gastrointestinal stromal tumors irrespective of KIT or PDGFRA mutation status. *Am J Pathol*. 2004;165(1):107–113.
74. Sato Y. Role of ETS family transcription factors in vascular development and angiogenesis. *Cell Struct Funct*. 2001;26(1):19–24.
75. Hewett PW, Nishi K, Daft EL, Clifford Murray J. Selective expression of erg isoforms in human endothelial cells. *Int J Biochem Cell Biol*. 2001;33(4):347–355.
76. Yuan L, Le Bras A, Sacharidou A, et al. ETS-related gene (ERG) controls endothelial cell permeability via transcriptional regulation of the claudin 5 (CLDN5) gene. *J Biol Chem*. 2012;287(9):6582–6591.
77. Furusato B, Tan SH, Young D, et al. ERG oncoprotein expression in prostate cancer: clonal progression of ERG-positive tumor cells and potential for ERG-based stratification. *Prostate Cancer Prostatic Dis*. 2010;13(3):228–237.
78. Park K, Tomlins SA, Mudaliar KM, et al. Antibody-based detection of ERG rearrangement-positive prostate cancer. *Neoplasia*. 2010;12(7):590–598.
79. Sun C, Dobi A, Mohamed A, et al. TMPRSS2-ERG fusion, a common genomic alteration in prostate cancer activates C-MYC and abrogates prostate epithelial differentiation. *Oncogene*. 2008;27(40):5348–5353.
80. Liu H, Shi J, Wilkerson M, Yang XJ, Lin F. Immunohistochemical evaluation of ERG expression in various benign and malignant tissues. *Ann Clin Lab Sci*. 2013;43(1):3–9.
81. Miettinen M, Wang ZF, Paetau A, et al. ERG transcription factor as an immunohistochemical marker for vascular endothelial tumors and prostatic carcinoma. *Am J Surg Pathol*. 2011;35(3):432–441.
82. Miettinen M, Wang Z, Sarlomo-Rikala M, Abdullaev Z, Pack SD, Fetsch JF. ERG expression in epithelioid sarcoma: a diagnostic pitfall. *Am J Surg Pathol*. 2013;37(10):1580–1585.
83. McKay KM, Doyle LA, Lazar AJ, Hornick JL. Expression of ERG, an Ets family transcription factor, distinguishes cutaneous angiosarcoma from histological mimics. *Histopathology*. 2012;61(5):989–991.
84. Santagata S, Ligon KL, Hornick JL. Embryonic stem cell transcription factor signatures in the diagnosis of primary and metastatic germ cell tumors. *Am J Surg Pathol*. 2007;31(6):836–845.
85. Wilkerson M, Lin F, Shi J. NANOG immunohistochemical expression in tumors [USCAP Abstract 1057]. *Mod Pathol*. 2012;25(suppl S2):251A.
86. Santagata S, Hornick JL, Ligon KL. Comparative analysis of germ cell transcription factors in CNS germinoma reveals diagnostic utility of NANOG. *Am J Surg Pathol*. 2006;30(12):1613–1618.
87. Ezeh UI, Turek PJ, Reijo RA, Clark AT. Human embryonic stem cell genes OCT4, NANOG, STELLAR, and GDF3 are expressed in both seminoma and breast carcinoma. *Cancer*. 2005;104(10):2255–2265.